GLIA

Ca^{2+}-dependent release of ATP from astrocytes affects Herpes simplex virus type 1 infection of neurons

Journal:	*GLIA*
Manuscript ID	GLIA-00056-2020.R1
Wiley - Manuscript type:	Original Research Article
Date Submitted by the Author:	n/a
Complete List of Authors:	Li Puma, Domenica; Catholic University, Institute of Human Physiology; Fondazione Policlinico Universitario A. Gemelli IRCCS Marcocci, Maria; Sapienza University of Rome, Department of Public Health and Infectious Diseases Lazzarino, Giacomo; UniCamillus - Saint Camillus International University of Health Sciences De Chiara, Giovanna; National Research Council, Institute of Translational Pharmacology Tavazzi, Barbara; Catholic University, Basic biotechnological sciences, intensivological and perioperative clinics; Fondazione Policlinico Universitario A. Gemelli IRCCS Palamara, Anna; Sapienza University of Rome, Department of Public Health and Infectious Diseases; San Raffaele Pisana, IRCCS, Telematic University Piacentini, Roberto; Catholic University, Department of Neuroscience; Fondazione Policlinico Universitario A. Gemelli IRCCS Grassi, Claudio; Catholic University, Department of Neuroscience; Fondazione Policlinico Universitario A. Gemelli IRCCS
Topics:	Astrocytes, Viral and bacterial infections, Neurodegenerative diseases
Techniques:	Immunocytochemistry, Molecular Neuroscience, Uptake and release of neurotransmitters
Key Words:	Astrocytes, Herpes simplex virus, ATP, P2Rs, GSK-3β

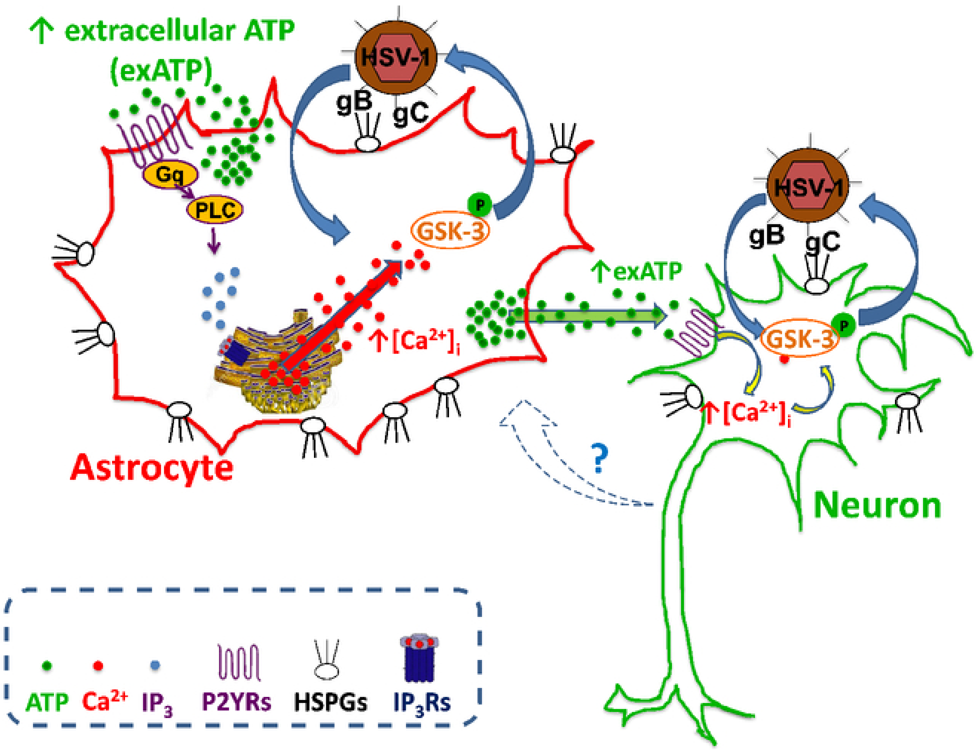

TOCI - Li Puma et al

56x42mm (300 x 300 DPI)

Ca^{2+}-dependent release of ATP from astrocytes affects Herpes simplex virus type 1 infection of neurons

Running title: Astrocytes affect neuronal HSV-1 infection

Domenica Donatella Li Puma[1,2], Maria Elena Marcocci[3], Giacomo Lazzarino[4], Giovanna De Chiara[5], Barbara Tavazzi[2,6], Anna Teresa Palamara[3,7], Roberto Piacentini[1,2]*, Claudio Grassi[1,2]

[1]Department of Neuroscience, Università Cattolica del Sacro Cuore, Rome, Italy

[2]Fondazione Policlinico Universitario A. Gemelli IRCCS, Rome, Italy

[3]Department of Public Health and Infectious Diseases, Sapienza University of Rome, Laboratory affiliated to Istituto Pasteur Italia - Fondazione Cenci Bolognetti

[4]UniCamillus - Saint Camillus International University of Health Sciences, Rome, Italy

[5]Institute of Translational Pharmacology, National Research Council, Rome, Italy

[6]Department of Basic biotechnological sciences, intensivological and perioperative clinics, Università Cattolica del Sacro Cuore, Rome, Italy

[7]San Raffaele Pisana, IRCCS, Telematic University, Rome, Italy

*Corresponding Author: Prof. Roberto Piacentini, Department of Neuroscience, Università Cattolica del Sacro Cuore, Rome, Italy. e-mail: roberto.piacentini@unicatt.it

Acknowledgments: This study has been supported by the Italian Ministry of Education University and Research (PRIN: 2017A9MK4R_004 to CG; PRIN: 2015W729WH_005 to ATP and GDC, PRIN: 20179JHAMZ_006 to GDC). Università Cattolica del Sacro Cuore contributed to the funding of this research project (to RP) and its publication.

Conflicts of interest: The authors declare no competing financial interests.

Word count: Abstract, 248; Introduction, 533; Materials and Methods, 2274; Results, 2958; Discussion, 1033; References, 2376; Figure legends, 1068; Number of figures, 7; Total word count: 10556

Abstract

Astrocytes provide metabolic support for neurons and modulate their functions by releasing a plethora of neuroactive molecules diffusing to neighboring cells. Here we report that astrocytes also play a role in cortical neurons' vulnerability to Herpes simplex virus type-1 (HSV-1) infection through the release of extracellular ATP. We found that the interaction of HSV-1 with heparan sulfate proteoglycans expressed on the plasma membrane of astrocytes triggered phospholipase C-mediated IP_3-dependent intracellular Ca^{2+} transients causing extracellular release of ATP. ATP binds membrane purinergic P2 receptors (P2Rs) of both neurons and astrocytes causing an increase in intracellular Ca^{2+} concentration that activates the Glycogen Synthase Kinase (GSK)-3β, whose action is necessary for HSV-1 entry/replication in these cells. Indeed, in co-cultures of neurons and astrocytes HSV-1-infected neurons were only found in proximity of infected astrocytes releasing ATP, whereas in the presence of fluorocitrate, an inhibitor of astrocyte metabolism, switching-off the HSV-1-induced ATP release, very few neurons were infected. The addition of exogenous ATP, mimicking that released by astrocytes after HSV-1 challenge, restored the ability of HSV-1 to infect neurons co-cultured with metabolically-inhibited astrocytes. The ATP-activated, P2R-mediated, and GSK-3-dependent molecular pathway underlying HSV-1 infection is likely shared by neurons and astrocytes, given that the blockade of either P2Rs or GSK-3 activation inhibited infection of both cell types.

These results add a new layer of information to our understanding of the critical role played by astrocytes in regulating neuronal functions and their response to noxious stimuli including microbial agents via Ca^{2+}-dependent release of neuroactive molecules.

Keywords: Astrocytes, Herpes simplex virus, ATP, P2Rs, GSK-3β

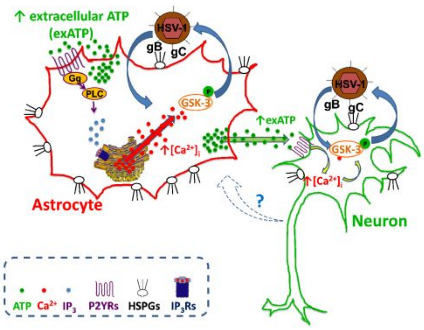

MAIN POINTS:

1) Ca^{2+}-dependent release of ATP from astrocytes affects neurons' vulnerability to HSV-1 infection

2) P2R-dependent GSK-3 activation is involved in HSV-1 entry/replication in both astrocytes and neurons

Introduction

Astrocytes are the most numerous subtype of glial cells within the central nervous system (CNS). Because their inability to fire action potentials, for many years they were considered passive elements only providing metabolic support for neurons and regulating the extracellular homeostasis of ions and selected molecules such as glutamate. To date, it is widely recognized that astrocytes play an active role in neuronal circuits by using intracellular Ca^{2+} fluxes to communicate with each other and interact with neighboring cells (Verkhratsky, 2019). In response to various stimuli, astrocytes generate transient elevation of cytosolic calcium mainly through activation of G_q protein-coupled receptors and production of inositol triphosphate (IP_3). IP_3 stimulates its receptors (IP_3Rs) located on the membrane of endoplasmic reticulum (ER) thus causing the release of Ca^{2+} with specific spatio-temporal patterns (Volterra et al., 2014; Bazargani & Attwell, 2016; Sherwood et al., 2017; Okubo et al., 2019) acting as intracellular second messenger. In astrocytes, these intracellular Ca^{2+} signals induce the release in the surrounding medium of soluble molecules including ATP, glutamate, and D-serine that modulate neuronal functions (Araque et al., 2014; Halassa & Haydon, 2010; Perea et al., 2009; Volterra & Meldolesi, 2005, Zonta et al., 2002). In particular, ATP, the predominant extracellular signaling molecule released from astrocytes (Cotrina et al., 2000), modulates neuronal excitability through the activation of different purinergic receptors, i.e., ionotropic P2XRs that are Ca^{2+}-permeable ligand-gated ion channel receptors, and metabotropic P2YRs that activate the phospholipase C (PLC)/IP_3 intracellular pathway (Fumagalli et al., 2003; Gordon et al., 2005; von Kügelgen & Hoffmann, 2016). Activation of ATP receptors leads to transient Ca^{2+} elevation that, in turn, triggers further release of ATP in an "ATP-induced ATP release" fashion sustaining and propagating intracellular Ca^{2+} elevation in adjacent astrocytes, a phenomenon also called “intracellular Ca^{2+} waves” (Wang et al., 2000).

Experimental evidence has revealed that astrocytes are partners of a bidirectional crosstalk with neurons regulating key neuronal functions, including synaptic transmission and plasticity. However, astrocytes do not only support neurons in their physiological functions, but they may be also involved in, or directly responsible for, their dysfunction. In fact, astrocytes have been reported to actively participate in the onset and progression of neurodegenerative diseases such as Alzheimer’s disease (AD), or cognitive decline in normal brain aging (see Phatnani & Maniatis, 2015; Verkhratsky, 2019). In this context, we recently demonstrated that astrocytes contribute to tau-oligomers synaptotoxicity through an altered release of extracellular ATP affecting synaptic transmission (Piacentini et al., 2017). Astrocytes were also reportedly involved in viral infections of CNS (Bender et al., 2012).

During the last decade we published a number of papers suggesting that that recurrent HSV-1 infection in the brain is a risk factor for AD. Specifically, HSV-1 triggers intracellular Ca^{2+} transients in neurons via activation of both IP_3Rs on ER and L-type voltage-gated Ca^{2+} channels (Ca_v1) on the plasma membrane (Piacentini et al., 2011). In the present study we demonstrated that astrocytes play a critical role in HSV-1 infection of neurons by a mechanism involving the Ca^{2+}-dependent extracellular release of ATP from infected astrocytes that activates P2YRs on the plasma membrane of neighboring neurons thus leading to IP_3- and Ca^{2+}-dependent activation of GSK-3β that is required for HSV-1 entry and replication in cells.

Material and Methods

Primary cultures of cortical neurons and astrocytes

Co-cultures of cortical neurons and astrocytes were obtained from wild type (WT) E18 C57/bl6 mice as previously described (Piacentini et al., 2015). Briefly, after removing brain, dissected cortices were incubated for 10 min at 37°C in phosphate buffered saline (PBS) containing trypsin-ethylenediaminetetraacetic acid (0.025%/0.01% w/v; Biochrom AG, Berlin, Germany) and the tissue was mechanically dissociated at room temperature [(RT), 23-25°C] with a fire-polished Pasteur pipette. The cell suspension was harvested and centrifuged at 235 × g for 2 min. Then, for co-cultures of neurons and astrocytes, the pellet was suspended in 88.8% minimum essential medium (MEM, Biochrom), 5% fetal bovine serum (FBS), 5% horse serum, 1% glutamine (2 mM), 1% penicillin–streptomycin-neomycin antibiotic mixture (PSN, Thermo Fisher Scientific, Waltham, MA, USA), and glucose (25 mM). Cells were plated at a density of 10^5 cells on 20-mm coverslips (for immunocytochemical studies) and 10^6 cells/well on 35-mm six-well plates (for Western blot experiments), precoated with poly-L-lysine (0.1 mg/ml; Sigma, St. Louis, MO, USA). Twenty four hours later, the culture medium was replaced with a mixture of 96.5%

Neurobasal medium (Thermo), 2% B-27 (Thermo), 0.5% glutamine (2 mM), and 1% PSN. After 72 h, this medium was replaced with a glutamine-free version of the same medium, and the cells were grown for 12 days before carrying-out experiments. Under these culture conditions, we had 14±3% MAP2-positive neurons and 78±3% of GFAP-positive cells. The mean density of neurons was 48±4 neurons/mm^2. For some experiments, 2 µM Cytosine arabinoside (Ara-C, Sigma) was added to the culture medium to inhibit the growth of glia. Addition of Ara-C to the culture medium did not significantly modify neuronal density.

For primary cultures of cortical astrocytes, the suspension of single cells (obtained as before) was suspended in a medium consisting of MEM with 3.7 g/L NaHCO3 and 1.0 g/L D-glucose, 5% FBS, 1% PSN and then plated at high density on 20-mm coverslips (for Ca^{2+} imaging and immunocytochemical studies) or 35-mm six-well plates for and High-Pressure Liquid Chromatography (HPLC) measures and western blot experiments. The culture the medium was changed within 24 h of seeding and twice weekly thereafter.

HSV-1 infection

HSV-1 (F strain, a wild-type strain) production was performed in VERO cells, as previously reported (De Chiara et al., 2010). Infection of cultured cells by HSV-1 was performed as previously described (Piacentini et al., 2011 and 2015). Ten-to-twelve days after plating (days in vitro, DIV), the cell culture medium was replaced with Neurobasal or MEM medium (for neurons or astrocytes, respectively), containing particles of HSV-1 [stock virus: 5 × 10^8 plaque forming units (PFU)/mL] at a multiplicity of infection (MOI) of 5, and cells were incubated for 1 h at 37 °C (adsorption period). After this time, the HSV-1-containing medium was removed and, after 2 washes in PBS, the cells were returned to the original medium and cultured for 24 h. HSV-1-infected cells were then studied by immunocytochemistry (see below) to identify infected cells. At the same time, the supernatants of infected cells were subjected to standard plaque assay to quantify virus production (Killington et al., 1991), as we did in our previous papers (Piacentini et al., 2015, De Chiara et al., 2019). In all the experiments, the effects observed in infected cells were compared with those obtained in mock-infected controls that had been exposed to the vehicle alone.

For HPLC experiments viral incubation was performed in Tyrode's solution containing (in mM): 150 NaCl, 4 KCl, 1 $MgCl_2$, 10 glucose, 10 HEPES, and 2 $CaCl_2$ (pH adjusted to 7.4 with NaOH).

Immunocytochemistry

Cortical neurons and astrocytes cultured for 10-12 DIV were infected with HSV-1 and then fixed with 4% paraformaldehyde (PFA) in PBS for 15 min at RT as described in Panella et al., 2016. After being permeabilized (10 min incubation with 0.3% Triton X-100 [Sigma] in PBS), the cells were incubated for 20 min with 0.3% bovine serum albumin in PBS to block nonspecific binding sites and then overnight at 4 °C with different pairs of the following antibodies: goat anti-HSV-1/2 (1:500; Bio-Rad, Hercules, CA), recognizing infected cell polypeptides – ICPs- and late structural virion antigens; mouse anti-ICP4 antibody (1:100; Santa Cruz, CA, USA); rabbit anti-Microtubule-associated protein 2 (MAP2; 1:500; Sigma); mouse anti-heparan sulfate proteoglycans (HSPGs, 1:500; UsBiological Salem, MA), rabbit anti-APP phosphorylated at Thr668 (pAPP, 1:100; Cell Signalling Technology Inc., Danvers, MA); mouse anti-Glial fibrillary acidic protein (GFAP, 1:500; Cell Signalling Technology); mouse anti-MAP2 (1:500; Immunological Sciences, Rome, Italy); rabbit anti-pGSK3 α /β (Tyr279/ Tyr216) (1:300; Signalway Antibody, College Park, MD). The next day, cells were incubated for 90 min at RT with a mixture of the following secondary antibodies: Alexa Fluor 546 donkey anti-mouse (1:1,000; Thermo); Alexa Fluor 488 donkey anti-rabbit (1:1,000; Thermo); Alexa Fluor 633 donkey anti-goat (1:1,000; Thermo); Alexa Fluor 488 donkey anti-mouse (1:1,000; Thermo); Alexa Fluor 546 donkey anti-rabbit (1:1,000; Thermo). Nuclei were counterstained with 4',6-diamidino-2-phenylindole (DAPI, 0.5 μ g/ml for 10 min; Thermo) and the cells were coverslipped with ProLong Gold anti-fade reagent (Thermo). Images (512 × 512 or 1024 × 1024 pixels) were acquired at 20× (625 × 625 μm^2), 40× (317 × 317 μm^2) or 60× (211 × 211 μm^2) magnification with a confocal laser scanning system (A1MP, Nikon, Tokyo, Japan) and an oil-immersion objective (N.A. 1.4). For some images, additional 2× magnification was applied. Fluorescent dyes were excited with diode lasers (405, 488, 546, and 633 nm). All experiments were repeated at least 3 times, and at least 10 randomly chosen microscopic fields were analyzed for each condition. For immunofluorescence quantification (e.g. HSPGs), overall fluorescence of maximum projection image from the confocal stacks was evaluated as sum of intensity in every pixel of the image. This value was then divided by the area in the field that was occupied by each cells that was automatically evaluated with a plugin of Image J software. Fluorescent dots that we recognized as unspecific staining were manually removed from the analysis.

Immunohistochemistry

For these experiments we used the mouse model of recurrent HSV-1 infection in the brain recently described and characterized in De Chiara et al. (2019) and Li Puma et al. (2019). Mice were inoculated with HSV-1 via lip scarification and after 6 weeks, when virus was likely gone in latency, they were subjected to two thermal stresses to induce viral reactivation. Two weeks after the last reactivation mice were deeply anesthetized with a cocktail of ketamine (100 mg/mL) and medetomidine (1 mg/mL) (ratio, 5:3) and transcardially perfused with 4% PFA, as described in Leone et al. (2019). Brains were then removed from the skull and post-fixed overnight at +4 °C, and finally transferred to a solution of sucrose (30% in PBS) for 2 days. Fixed tissues were embedded in OCT and coronal sections (40-µm thick) were obtained with a SLEE cryostat type MEV (SLEE Medical, Mainz, Germany) at -20 °C and stored in a cryoprotectant at -20 °C. After three rinses in PBS, sections were incubated in a blocking solution containing 1% bovine serum albumin, 10% normal goat serum, and 0.5% Triton X-100 for 1h a RT. Double labeling for GFAP and viral glycoprotein B (gB) was performed on a one-in-six series of equidistant (240 µm between sections) free-floating sections by using the following antibodies: mouse anti-GFAP antibody (1:300; Cell Signaling); rabbit anti-gB antibody (1:100; Santa Cruz Biotechnology). The fluorescent secondary antibodies Alexa Fluor 488 donkey anti-mouse (1:500); Alexa Fluor 546 donkey anti-rabbit (1:1,000) were then used. Finally, cell nuclei were counterstained with DAPI (0.5 µg/mL) and the sections were mounted on glass slides and coverslipped with ProLong Gold antifade reagent. Confocal stacks of images were acquired at 40× magnification with a confocal laser scanning system (A1MP, Nikon, Tokyo, Japan) and an oil-immersion objective (N.A. 1.4).

Western Blot

Western blot (WB) analysis was performed as described previously (Gulisano et al., 2019). Infected or mock-infected cortical cultures (10-12 DIV) were washed twice with PBS and scraped in cold RIPA buffer containing 1 mM phenylmethylsulfonyl fluoride, phosphatase and protease inhibitor mixtures (Sigma). After incubation for 15 min on ice, cellular suspensions were centrifuged (10,000 × *g* for 30 min at 4 °C) and the supernatants were collected and assayed to determine their protein concentration (Bradford protein assay, Bio-Rad). Equivalent amounts of proteins were loaded onto either 8 or 10% tris-glycine polyacrylamide gels for electrophoretic separation, and then electroblotted onto nitrocellulose membranes for Western blot analysis. Membranes were blocked with 5% nonfat dry milk in tris-buffered saline containing 0.1% Tween-20 for 1 h at RT and incubated with primary antibodies: goat anti-HSV-1; mouse anti-ICP4 antibody; rabbit anti-gB antibody; rabbit polyclonal anti-pGSK3 α /β (Tyr279/Tyr216); rabbit polyclonal anti- total GSK-3β (Cell Signaling), all used at a final concentration of 1 µg/mL. After incubation with appropriate secondary horseradish peroxidase-conjugated antibodies (1:2,000; Cell Signaling), visualization was performed with ECL plus (GE Healthcare, Amersham Place, Buckinghamshire) using either UVItec Cambridge Alliance. Molecular weights for immunoblot analysis were determined using BenchMark™ Pre-Stained Protein Ladder (Thermo). Densitometric analysis was carried out with Image J or UVItec softwares. Experiments were repeated at least 3 times.

Confocal Ca^{2+} imaging

Confocal Ca^{2+} imaging was performed as previously described (Piacentini et al., 2011, 2014 and 2017). Briefly, either cultured cortical astrocytes or neurons were incubated for 30 min at 37°C with the Ca^{2+} sensitive fluorescent dye Fluo-4 AM (2.5 µM, Thermo) dissolved in Tyrode's solution (150 mM NaCl, 4 mM KCl, 1 MgCl2, 10 mM glucose, 10 mM (4-(2-hydroxyethil)-1-piperazineethanesulfonic acid (HEPES), and 2 mM CaCl2; pH adjusted to 7.4 with NaOH), and then maintained in fresh Tyrode's solution at RT for 20 min to allow dye de-esterification. Cells were then studied by means of an inverted confocal microscope (TCS-SP2; Leica). Fluo-4 was excited at 488 nm and the emission signal was collected within a spectral window ranging from 500 to 535 nm. Intracellular Ca^{2+} signals were studied under continuous perfusion and quantified in terms of $\Delta F/F = (F_t - F_{pre})/(F_{pre} - F_{bgnd})$, where F_t is the mean of fluorescence intensities measured at a given time (t) in a region of interest (ROI) traced around each cell body; F_{pre} is the basal fluorescence intensity in this ROI; and F_{bgnd} is background fluorescence intensity measured in an area of the imaged field lacking dye-filled structures. Neuron depolarization was obtained by perfusing cells for 10 s with a modified Tyrode's solution in which KCl concentration was elevated to 50 mM (and NaCl was accordingly reduced to 104 mM to assure iso-osmolarity of the solution). Continuous perfusion was achieved via a gravity-based system and a vacuum pump. The acquisition frame rate was 0.2-0.5 Hz depending on the experiment made. No bleaching was observed under these experimental conditions. Measures were performed at RT.

High performance liquid chromatography (HPLC) measurements

HPLC measurements were performed as described in Piacentini et al., 2017, with some modifications. Briefly, astrocytes were cultured in 30-mm wells and treated for 1 hour with HSV-1 or vehicle in Tyrode's solution. At the end of treatment Tyrode's solution was withdrawn from each well and samples were treated with $HClO_4$ 14% (v:v) to inactivate virus. Acid deproteinized samples were centrifuged at 13,000 rpm for 10 minutes at 4°C. Supernatants were then neutralized with 5 M K_2CO_3 and stored at -20°C overnight in order to optimizing potassium perchlorate precipitation. After centrifugation at 13,000 rpm for 10 minutes at 4°C, neutralized samples were filtered through a 0.45-µm HV-Millipore filter and then loaded onto the HPLC column and analyzed to determine concentrations of ATP, ADP, glutamate (Glu), glutamine (Gln), and serine (Ser, as sum of L- and D- isomers). The two nucleotides were separated and quantified according to an ion-pairing HPLC method previously set up (Tavazzi et al., 2005), whilst the amino acids were analyzed as ortophtalaldehyde (OPA) derivatives using a different method with pre-column derivatization (Amorini et al., 2012, 2017). For both analyses, the HPLC apparatus (Thermo) consisted of a P4000 quaternary pump system, an AS3000 autosampler and a highly sensitive UV6000LP photodiode array detector equipped with a 5 cm light path flow cell and set up between 200 and 400 nm wavelength. Data acquisition and analysis were performed by a PC using the ChromQuest® software package provided by the

HPLC manufacturer. Separation of the various compounds was carried out using a Hypersil C-18; 250 × 4.6 mm, 5 μm particle size thermostated at 10°C for nucleotides separation and at 21°C for amino acids separation. Species identification and quantification in deproteinized samples of extracellular medium was determined by matching retention times, peak areas and adsorption spectra of those of freshly prepared ultrapure standards. If needed, cochromatograms were performed by adding proper standards with known concentration to the medium samples. The concentrations of ATP and ADP were determined at 260 nm wavelength and those of OPA-derivatized amino acids were calculated at 338 nm wavelength.

Statistics

Statistical comparisons were performed with Sigmaplot 14 software. All data were expressed as mean ± standard error of the mean (SEM) and followed normal distribution, as assessed by the same software. In order to assess whether HSV-1 infection significantly affected the measured parameters, the two-tailed Student's t-test was used. One-way ANOVA with Bonferroni *post hoc* test was used for multiple comparisons. For experiments that included fewer than 10 observations (e.g., densitometric analysis of western blotting data), or for non-normally distributed data, the Mann-Whitney Rank Sum Test was used. The level of significance was set at 0.05. In all experiments, the operators were blind to the study conditions.

Ethics Statement

All animal procedures were approved by the Ethics Committee of Università Cattolica and were fully compliant with Italian (Ministry of Health guidelines, Legislative Decree No. 116/1992) and European Union (Directive No. 86/609/EEC) legislation on animal research. Animals were supplied by the Division of Animal Resources of Università Cattolica.

Results

Neurons closer to infected astrocytes are more susceptible to HSV-1 infection

First, we studied the ability of HSV-1 to infect cortical neurons co-cultured with astrocytes by exposing co-cultures to 5 multiplicity of infection (MOI) HSV-1 for 1 h, that was the adsorption time (see also Methods). After this time period cells returned to their standard culture medium for further 24 h (defined as time post-infection, p.i.). At the end of this protocol, we assessed the immunoreactivity of neurons (identified by expression of the neuron-specific cytoskeletal protein MAP2) for HSV-1 by using the anti-HSV-1 antibody recognizing various viral proteins (infected cell polypeptides – ICPs- and late structural virion antigens). In agreement with our previous reports (Piacentini et al., 2011, 2015), we found immunoreactivity for HSV-1 in both cultured neurons and astrocytes. However, the percentage of HSV-1-positive neurons on the total number of neurons varied depending on the presence or not of infected glial (i.e., HSV-1-positive and MAP2-negative) cells. In particular, we found that about 60% of all HSV-1$^+$ neurons were localized at a distance ≤ 25 µm from the soma of the nearest infected astrocyte (**Figure 1a-d**) with a mean distance of all infected neurons of 59.8±4.8 µm (*n*=148 infected neurons out of 317 total neurons counted in at least 10 random fields for experiment). On the contrary, HSV-1-negative neurons were found farer from infected astrocytes (206.9±6.9 µm, *n*=169 out of 317; **Figure 1d-e**). Similar results were also obtained studying immunoreactivity for the early viral protein ICP4 to recognize HSV-1-infected cells. ICP4 is an immediate early viral protein whose synthesis is required for productive infection and its expression and distribution within cell nuclei changes during the time p.i. depending on viral DNA replication (Randall & Dinwoodie, 1986). The percentage of ICP4-positive neurons on the total number of neurons was very high (78.7±5.9%) in the proximity (≤100 µm) of infected astrocytes and was significantly lower (12.3±5.5%) at a distance > 200 µm from them ($p=2.1\times10^{-11}$ assessed by two-tailed Student's *t*-test; **Supplementary Figure 1a-c**). These findings were also supported by results of *ex vivo* studies carried out on brain slices of a mouse model of HSV-1 infection and recurrent reactivations (De Chiara et al., 2019). Specifically, in the granular cell layer of the dentate gyrus immunoreactivity for the viral glycoprotein B (gB), detecting active viral replication, was observed in neurons only when their cell bodies were close to infected astrocytes (**Supplementary Figure 1d,e**).

These observations suggested us that the proximity of infected astrocytes to neurons might promote the latter's infection by HSV-1, although the possibility that hot spots of infection reach nearby astrocytes and neurons can not be excluded. To test our hypothesis we inhibited astrocyte metabolism by using fluorocitrate (FC), a mitochondrial inhibitor specific for glial cells that blocks their Krebs cycle (Clark, 1991; Voloboueva et al., 2007) thus precluding viral replication and propagation of infection that exploit the metabolic resources of host cells (Ackermann, 1951; Ackermann & Kurtz, 1952; Vastag et al., 2011). At DIV 12 co-cultures of cortical astrocytes and neurons were treated with 200 µM FC starting from 30 min prior to HSV-1 challenge and during the 1-h adsorption time. After 24 h cells were collected for WB analyses. The anti-HSV-1 antibody revealed very faint band at ~ 100 KDa in FC-treated cultures compared to infected FC-untreated ones in which the band corresponding to HSV-1 was very intense ($p<0.005$; assessed by Mann-Whitney Rank Sum Test; **Figure 2a,b**). These data were also confirmed by assessment of viral titre in the supernatants of infected cells that revealed lower levels of PFU/mL ($4.5\pm0.6 \times 10^2$ PFU/mL) in FC-treated cultures than in FC-untreated ones ($4.9\pm2.2 \times 10^3$ PFU/mL ($p=0.005$; assessed by Mann-Whitney Rank Sum Test; **Figure 2c)**.

We previously demonstrated that challenging neurons with HSV-1 triggers intracellular Ca^{2+} transients mainly due to activation of IP_3Rs and Ca_v1 channels (Piacentini et al., 2011). Here we repeated these experiments and demonstrated that in co-cultures treated with FC, virus was ineffective in inducing significant Ca^{2+} signals in neurons (**Figure 2d**). Nevertheless, neurons responded to membrane depolarization induced by extracellular application of 50 mM KCl with Ca^{2+} transients whose amplitude was similar to that observed in control, FC-untreated neurons (**Figure 2e**).

Similar results were also obtained by inhibiting astrocytic growth with the addition of 2 µM of Ara-C to the culture medium of neuronal cultures from DIV 1 to 4 (Piacentini et al., 2008). At DIV 12, these neuron-enriched cultures were challenged with either HSV-1 (5 MOI) or vehicle (mock-infected cells) for 1 h and subsequently cultured for 24 h p.i. as described above. As revealed by WB experiments a high infection was observed in infected primary cultures of astrocytes, whereas a very slight HSV-1-immunoreactivity was obtained in neuronal cultures treated with Ara-C (**Supplementary Figure 2a,b**). In a previous study (De Chiara et al., 2016) we reported that a more efficient infection of neurons could be obtained at a higher HSV-1 MOI (i.e., 10). As for FC, in the absence of astrocytes neurons produced very small intracellular Ca^{2+} signals in response to HSV-1 though their ability to produce Ca^{2+} transients following KCl-induced membrane depolarization was not significantly affected (**Supplementary Figure 2c,d**). All together, these data strongly support the primary role of astrocytes in the Ca^{2+} signals triggered by HSV-1 exposure in neurons and suggest that the presence of functional astrocytes increases the probability that neurons are infected by HSV-1.

Astrocytes express more receptors for initial HSV-1 binding than neurons

It is known that HSV-1 infection starts with the interaction of glycoproteins present on the viral envelope (gC and gB) with the HSPGs expressed on the cell membrane (Shukla & Spear, 2001; Akhtar & Shukla, 2009; Tiwari et al., 2015, Lathe and Haas, 2016). Infection continues with high-affinity binding of the viral gD glycoprotein to one of the gD receptors, promoting recruitment of gB, gH and gL and then the viral fusion with host plasma membrane (Agelidis & Shukla, 2015). We hypothesized that cultured astrocytes are more susceptible than neurons to HSV-1 infection because they express more receptors needed for HSV-1 binding. This hypothesis is in agreement with literature reports demonstrating different binding of HSV-1 to neurons and glial cells (Vahlne et al., 1978; Vahlne et al., 1980). To address this issue, we compared the immunoreactivity of cultured astrocytes and neurons for an antibody recognizing HSPGs. We found that GFAP-positive astrocytes exhibited a mean HSPG density (immunofluorescence signal/surface area) slightly higher than MAP2-positive neurons (+1.6±0.2 fold; **Figure 3a-c**). If we consider that in our cultures astrocytes have a surface area about 10-15 times larger than neurons, these data suggest that the overall expression of HSPG in astrocytes is about 15-20 times greater than in neurons.

Cultured astrocytes challenged with HSV-1 exhibit increased intracellular Ca^{2+} transients and ATP release in the culture medium

We then wondered how astrocytes may contribute to neuronal HSV-1 infection. Several reports indicate that astrocytes modulate neuronal functions through Ca^{2+}-dependent release of neuroactive molecules including purines (e.g. ATP), glutamate, D-serine and TNF-α (Araque et al., 1998; Fields & Burnstock, 2006; Jourdain et al., 2007; Perea & Araque, 2010; Piacentini et al., 2017; Zorec et al., 2017).

Therefore, we checked whether HSV-1 also induced intracellular Ca^{2+} transients in cultured cortical astrocytes. These cells exhibited basal Ca^{2+} activity characterized by spontaneous transients with mean frequency of 1.7±0.2 spikes/min and mean amplitude of 2.7±1.0, expressed as ΔF/F. Soon after HSV-1 challenge both frequency and amplitude of Ca^{2+} transients increased significantly to 2.3±0.2 spikes/min and 7.4±0.5 ΔF/F, respectively ($p=0.039$ and $p=9.5\times10^{-5}$, assessed by Student's *t*-test; **Figure 4a-c**), and these effects were reverted by cell washout with HSV-1-free Tyrode's solution (**Figure 4a**).

In astrocytes, intracellular calcium transients regulate gliotransmitter release. Our previous findings indicate that basal Ca^{2+} levels/signals exhibited by cultured astrocytes were sufficient to trigger the release of ATP, glutamate, glutamine and serines in the extracellular medium (Piacentini et al., 2017). We then checked whether this release is affected by the increase in intracellular Ca^{2+} concentration induced in astrocytes by HSV-1 during the adsorption step. To address this question, supernatants of cultured astrocytes challenged for 1 hour with HSV-1 or vehicle alone were analyzed by HPLC. To avoid any possible confounding effects exerted by components of the culture medium, the HSV-1 adsorption was carried out in Tyrode's solution and gliotransmitters were measured in the conditioned medium (see "Methods"). In agreement with the increase of intracellular Ca^{2+} signals in astrocytes, we found that HSV-1 application significantly increased the amount of gliotransmitters released extracellularly and, in particular, ATP (from 9.9±1.1 nM [*n*=10] to 38.7±6.0 nM [*n*=10], $p=9.9\times10^{-5}$ assessed by Student's t test), ADP (14.2±2.6 [*n*=10] vs. 34.4±6.3 nM [*n*=10], p=0.006) and glutamate (1.3±0.2 [*n*=9] vs. 2.5±0.3 µM [*n*=9], p=0.007) (**Figure 4d).**
Notably, astrocytes do not release ADP that is produced from ATP by ectonucleotidases (Burnstock, 2007). This means that the overall ATP released from astrocytes may be quite higher than that we measured.

HSV-1-induced ATP release from astrocytes is prevented by the blockade of P2Y receptors

To examine whether activation of the PLC/IP_3 intracellular pathway induced by the binding of extracellular ATP to P2YRs contributed to intracellular Ca^{2+} transients triggered by HSV-1 in astrocytes, calcium imaging experiments were repeated in the presence of the selective inhibitor of phospholipase C, U-73122 (5 µM). This compound completely abolished the spontaneous activity that astrocytes exhibited before HSV-1 exposure as well as the HSV-1-induced Ca^{2+} transients in these cells (*n*=88 cells analyzed), confirming the involvement of metabotropic P2YRs in this effect (**Supplementary Figure 3a**).

Suramin, a symmetrical polysulfonatenapthylamine derivative of urea, is a blocker of both ionotropic and metabotropic P2Rs (Aguilar et al., 1999). Addition of 200 µM suramin to the culture medium of astrocytes during the adsorption period of HSV-1 abolished the virus-induced increase in gliotransmitters release. In fact, ATP levels in the supernatants of astrocytes challenged for 1 h with HSV-1 in the presence of suramin were 10.1±1.5 nM *vs*. 44.1±11.3 nM of suramin untreated HSV-1-infected astrocytes (p=0.035, assessed by Mann-Whitney Rank Sum test). No significant effects were exerted by suramin on the release of ATP from cells treated for 1 h with vehicle alone (10.1±2.2 nM; p=0.9; **Supplementary Figure 3c**). Notably, suramin also almost completely abolished intracellular Ca^{2+} transients induced by HSV-1 exposure in astrocytes (**Supplementary Figure 3b**). Collectively, these results strongly suggest the involvement of a Ca^{2+} dependent "ATP-induced ATP release" in the effects provoked by HSV-1.

Several studies also demonstrated the important role of P2Rs in mediating viral infections (Pacheco et al., 2014; Séror et al., 2011; Swartz et al., 2015; Tovar-y-Romo et al., 2013). We then checked whether activation of P2Rs was involved in HSV-1 infection of co-cultures of cortical astrocytes and neurons. The addition of 200 µM suramin to the culture medium 30 min before cell challenge with HSV-1 and throughout the adsorption period significantly decreased infection as documented by the reduction of the viral titre in the supernatants of suramin-treated cultures evaluated 24 h p.i. ($2.7\pm0.6\times10^{1}$ PFU/mL *vs.* $4.9\pm2.2\times10^{3}$ PFU/mL of untreated infected cultures; $p<0.01$; assessed by Mann-Whitney Rank Sum Test).

Extracellular ATP contributes to HSV-1 infection of neurons

Data shown so far indicated that activation of P2Rs is necessary for HSV-1 infection of co-cultures of neurons and astrocytes. Therefore, it is reasonable to hypothesize that extracellular ATP released from astrocytes after challenge with HSV-1 may be involved in HSV-1 infection of both cell populations. To test this hypothesis, we treated co-cultures of cortical astrocytes and neurons with FC, that inhibits metabolism of astrocytes only, thus making them unaffected by virus and unable to allow its replication. We first verified that, in pure cultures of astrocytes, the addition of FC affected extracellular HSV-1-induced ATP release, that was significantly reduced by about 40% (22.3±7.9 *vs*. 38.7±6.0 nM in FC-untreated cultures; $p<0.05$). We then added exogenous ATP (ex-ATP, 100 µM) to the culture medium of FC-treated cells during the 1-h adsorption period of HSV-1 to mimic ATP released from astrocytes challenged with HSV-1, and assessed neuronal infection after 24 h. For these experiments we chose the concentration of ex-ATP determining Ca^{2+} transients whose amplitude was similar to that observed after cell challenge with HSV-1 (Piacentini et al., 2017). The addition of 100 µM ATP to FC-treated co-cultures of neurons and astrocytes restored neuronal HSV-1 infection, as suggested by: i) immunofluorescence experiments demonstrating that the percentage of neurons far from infected astrocytes and immunoreactive for ICP4 expression raised from 8.5±1.8% to 71.5±12.1% of total neurons in FC-treated cultures following exposure to ex-ATP ($p=0.001$ *vs*. HSV-1 + FC; assessed by Bonferroni *post hoc* test; **Figure 5a-c**); ii) Western Blot experiments showing that intensity of the band corresponding to HSV-1 significantly increased in FC-treated cultures exposed to ex-ATP respect to unexposed ones ($p<0.05$ assessed by Mann-Whitney Rank Sum Test; **Figure 5d,e**); iii) determination of viral titre in the supernatants that was $2.2±0.5 \times 10^3$ in FC+ATP-treated cultures *vs*. $4.5±0.6 \times 10^2$ PFU/mL in FC-treated cultures ($p<0.001$ assessed by Mann-Whitney Rank Sum Test; **Figure 5f**). Viral titre and the intensity of the band observed in WB experiments in FC-treated cultures were smaller than in FC-untreated cultures probably because in the former experimental condition only neurons likely contributed to HSV-1 infection and virus replication, given that astrocytes were metabolically inhibited. In our cultures, the neurons to astrocytes ratio was about of 1:6, therefore it is reasonable to expect intensity values much smaller than those observed in co-cultures of functional neurons and astrocytes.

In FC-treated co-cultures infected in the presence of 1 µM exATP no significant differences were found with respect to FC-treated ones. In fact, in this condition the viral titre was 6.1±5.2 $\times 10^2$ pfu/mL (p=0.52 *vs*. FC-treated ones).

Purinergic receptors mediate Ca^{2+}-dependent activation of GSK-3 by phosphorylation at Tyr216

We then investigated the molecular pathway underlying the ATP-mediated HSV-1 infection of astrocytes and neurons. We previously reported that HSV-1 application induced APP phosphorylation at Thr668 ($pAPP^{T668}$) as soon as 10 min after HSV-1 exposure and that this effect depended on IP_3-mediated Ca^{2+} release from ER, as demonstrated by using the IP_3R inhibitor, 2-APB (Piacentini et al., 2011). It is known that Thr668 of APP and its C-terminus fragments is substrate for several kinases including the glycogen synthase kinase (GSK)-3, the c-Jun N-terminus kinase (JNK) and Cyclin-dependent kinase 5 (Cdk5) (Aplin et al., 1996; Piacentini et al., 2015; Pierrot et al., 2006).

To determine which kinase was activated after HSV-1 application we studied $pAPP^{T668}$ in neurons in the presence of specific kinase inhibitors added 30 min before and during HSV-1 adsorption. We found that the increase in $pAPP^{T668}$ observed 10 min after HSV-1 challenge was markedly reduced by 10 µM SB216763, an ATP-competitive inhibitor of GSK-3 (-58%; $p<1\times10^{-6}$, assessed by ANOVA followed by Bonferroni *post hoc*; **Supplementary Figure 4a-d**). The inhibition of Cdk5 (by roscovitin) and JNK (by inhibitor "I") exerted milder effects (-29%; $p<1\times10^{-6}$ and -13%; p>0.05, respectively; **Supplementary Figure 4e**).

These results strongly suggest that HSV-1 mainly induces activation of GSK-3. GSK-3α/β is a Ser/Tyr kinase that is inhibited by phosphorylation at Ser21/9 and activated by phosphorylation at Tyr276/216. Since SB216763 has been reported to act mainly on tyrosine than on serine, we studied activatory GSK-3 phosphorylation at Tyr276/216 (pGSK-3) by immunocytochemistry.

As expected, 10 min after HSV-1 application we observed a significant increase of pGSK-3 in astrocytes and neurons (+115±8% and +54±2% *vs*. controls, respectively; p<0.001 for both, assessed by One-way ANOVA followed by Bonferroni *post hoc* test (**Figure 6a-i**). These increases were almost completely abolished by the presence of 200 µM suramin in the culture medium (**Figure 6c,d and 6g,i**; p<0.001 *vs*. HSV-1) thus indicating that P2YRs are involved in HSV-1-induced GSK-3 activation in both neurons and astrocytes. The increase of pGSK-3 in neurons was also abolished by the IP_3R blocker, 2-APB (**Figure 6i**), thus indicating its dependence on Ca^{2+} release from ER, likely due to the PLC/IP_3 pathway activation after ATP binding to P2YRs. Finally, to check whether functional astrocytes are needed for the HSV-1-induced GSK-3 activation in neurons, we repeated these experiments in co-cultures of neurons and astrocytes after FC treatment. No significant increases of pGSK-3 were observed in neurons after HSV-1 exposure under this experimental condition (**Figure 6h,i**).

Western blot analyses performed on lysates of HSV-1-challenged astrocytes treated with either FC or suramin further confirmed that GSK-3β activation by phosphorylation at Tyr216 depended on the ATP-induced P2Rs activation **(Figure 6j,k)**. In fact, both treatments reduced pGSK-3β^{Y216} levels by 40% with respect to HSV-1 alone without affecting total protein levels ($F_{2,8} = 6.2$; $p<0.05$).

GSK-3 activation is involved in HSV-1 binding/entry

We hypothesized that the early GSK-3 activation occurring during cell challenge with HSV-1 may play a role in virus entry/replication into the cells following its binding to HSPGs. To test our hypothesis, we inhibited the kinase by SB216763 (10 μM) 30 min before and during all the time of virus adsorption and evaluated infection after 24 h by assessment of viral titer and immunoreactivity for anti HSV-1. In SB216763-treated cultures we found no or very few HSV-1 immunoreactive cells (7.2±2.5% of total cells), along with reduced levels of PFU in the supernatants (viral titre: 6.4±3.5 ×10^2 PFU/mL) respect to cultures of astrocytes and neurons infected without GSK-3 blockade; **Figure 7a,b,d**). Notably, cell treatment with SB216763 performed only after viral adsorption (and maintained for all the 24 h p.i.) did not affect the ability of HSV-1 to establish infection (the viral titre being 4.3±2.9 ×10^3 PFU/mL at 24 h p.i.; **Figure 7c,d**), thus indicating that GSK-3 activation influences viral infection only during the adsorption period. These findings were also supported by consistent results obtained by Western Blot experiments in which a significant reduction of the expression of ICP4 (-65%; $p<0.05$) was observed respect to the untreated co-cultures of astrocytes and neurons (**Figure 7e,f**).

Collectively, these findings suggest the involvement of GSK-3 activation in viral penetration and/or the transport of viral capsids to the nucleus, and the consequent cell infection.

Discussion

Within the context of the complex crosstalk between astrocytes and neurons, with the formers markedly affecting activity and functions of the latters, here we demonstrated that astrocytes play a critical role in neurons' vulnerability to HSV-1 infection. In previous studies we documented that HSV-1 induced intracellular Ca^{2+} signals triggered by its binding with HSPGs, as demonstrated by cell treatment with heparinase III or virus treatment with heparin (Piacentini et al., 2011). Therefore, here we report that HSV-1 binding to HSPGs of astrocytes induces PLC-mediated IP_3-dependent intracellular Ca^{2+} increase determining an extracellular release of ATP. ATP binds and activates P2YRs located on the membrane of astrocytes themselves that, in turn, amplify IP_3-dependent elevation of intracellular Ca^{2+} leading to the release of further ATP that may diffuse to adjacent neurons thus activating the same pathway in these cells. Once elevated, Ca^{2+} promotes activation of GSK-3β (by phosphorylation at Tyr216) whose action is fundamental to promote viral entry and/or viral capsids transport to the nucleus. This pathway is probably shared by neurons and astrocytes, given that both suramin (a blocker of purinergic receptors) and SB216763 (a blocker of GSK-3) inhibited infection in our co-cultures. The ability of herpes simplex viruses to induce a transient increase of intracellular Ca^{2+} through the production of IP_3 and activation of the specific receptors on ER membrane, needed for virus entry, was reported by Cheshenko and colleagues (Cheshenko et al., 2003, 2013 and 2018). Moreover, the same group also demonstrated that fusion between HSV-1 and cell membrane triggers phosphorylation at tyrosine residues of several cellular proteins 5-10 min after virus challenge (Qie et al., 1999), in agreement with our data about GSK-3.

We found that astrocytes showed a greater susceptibility to HSV-1 infection than neurons and this likely depends on their greater expression of HSPGs that are the first binding sites for viral particles. This interpretation is in line with literature data indicating that glial cells express more selective receptors for HSV-1 than neurons, which is reflected in a greater HSV-1 adsorption (Vahlne et al., 1978; Vahlne et al., 1980). Some studies reported that the susceptibility to HSV-1 infection, especially in human neuronal cells, depends on the presence of a specific ER protein, the UNC-93B known to be required for tool-like receptor (TLR) 3, TLR7, TLR8 and TLR9 responses to pathogens like bacteria and viruses (Casrouge et al., 2006; Lafaille et al., 2012). However, if this protein is also involved in IP_3-dependent Ca^{2+} release from ER is not known yet. Interestingly, in line with our present and published data (Li Puma et al., 2019), human astrocytes and neural stem cells were found to be more permissive to HSV-1 than neurons and oligodendrocytes, independently on UNC-93B expression (Lafaille et al., 2012).

Here we provide novel evidence that astrocytes contribute to and promote HSV-1 infection of neurons by fueling neurons of extracellular ATP that activates the P2R-mediated PCL/IP_3-dependent pathway leading to GSK-3 activation. In fact, in the absence of functional astrocytes, neurons are less infected even if able to generate depolarization-induced intracellular Ca^{2+} transients, but exogenous application of ATP at a concentration suitable to activate P2YRs (Juaristi et al., 2018) and to induce a significant increase of intracellular Ca^{2+} levels is sufficient for productive HSV-1 infection of neurons.

The involvement of P2Rs in infection of both neurons and astrocytes was determined pharmacologically by inhibiting these receptors with suramin and the role of ER-dependent Ca^{2+} release was demonstrated by using the IP_3R blocker 2-APB, both treatments significantly decreasing infection. The effects of suramin in preventing HSV-1 adsorption and virion attachment had been reported in Vero cells (Aguilar et al., 1999) although the underlying molecular pathway was not identified. Here we demonstrate that suramin interrupts the GSK-3-mediated pathway leading to the viral entry/replication in cells by avoiding the ATP-dependent activation of P2Rs.

This pathway seems to be also shared by cells of the peripheral nervous system (PNS), such as trigeminal ganglia neurons. In fact, even if HSV-1 infection mainly involves sensory neurons (Wilkinson et al., 1999; Zerboni et al., 2013) where the virus is able to establish a life-long latent infection, during the periodic reactivation of alpha herpesviruses (including HSV-1) replicating virus has also been reported to infect satellite glial cells (Athmanathan et al., 2001). Interestingly, it was reported that HSV-1 infection enhances

ATP-dependent intercellular Ca^{2+} waves among neurons and satellite glial cells and that suramin significantly reduces these signals (Goto et al., 2017; Warwik & Hanani, 2016).

Heparin, known to preclude HSV-1 binding to the cell membrane, was also reported to inhibit GSK-3β activation in N2a cells (Colombres et al., 2008), further supporting a role for this kinase in HSV-1 binding/entry. The role of GSK-3 in mediating infection/replication in several cell types was also reported for other viruses including hepatitis C virus (Sarhan et al., 2017), Herpes MHV-68 virus (Taylor et al., 2016), Virulent Porcine Epidemic Diarrhea virus (Kong et al., 2016), Newcastle disease virus (Kang et al., 2017), Corona virus (Wu et al., 2009), Venezuelan Equine Encephalitis virus (Kehn-Hall et al., 2012), and HIV (Guendel et al., 2014), indicating that this is a common intracellular pathway involved in viral infections.

Data reported here about the role of glia in mediating HSV-1 infection of neurons may represent an intriguing paradox if considering the recognized role of glial cells in brain protection from pathogens (Bender et al., 2012). Glial response to insults is reactive gliosis leading to release of a wide variety of extracellular molecules, including cytokines (such as interleukin-6 and transforming growth factor-β) with known neuroprotective potential (Sofroniew, 2009). However, in the case of HSV-1 we found that, at least *in vitro*, astrocytes concur to productive infection of neurons rather than protecting them.

Finally, our recent findings indicate that HSV-1 infection and recurrent reactivations in the mouse brain produce an AD-like phenotype characterized by intracellular accumulation of AD hallmarks including Aβ and phosphorylated tau, and inhibition of adult neurogenesis, that are associated with cognitive impairment (De Chiara et al., 2019; Li Puma et al., 2019). Interestingly enough, the results of this work also prompt future studies aimed at determining the specific contribution of astrocytes to the development of this AD-like phenotype because of their active role in favoring and spreading the infection of neurons.

Data Availability Statement

Data supporting the findings of this study are available from the corresponding authors, upon reasonable request.

References

1. Ackermann, W.W. (1951). The relation of the Krebs cycle to viral synthesis. II. The effect of sodium fluoroacetate on the propagation of influenza virus in mice. *Journal of Experimental Medicine*, 93(6):635-642. https://doi.org/10.1084/jem.93.6.635
2. Ackermann, W.W., & Kurtz, H. (1952). A new host-virus system. *Proceedings of the Society for Experimental Biology and Medicine*, 81(2):421-423. https://doi.org/10.3181/00379727-81-19897
3. Agelidis, A.M., & Shukla, D. (2015). Cell entry mechanisms of HSV: what we have learned in recent years. *Future Virology*, 10(10):1145-1154. https://doi.org/10.2217/fvl.15.85
4. Aguilar, J.S., Rice, M., Wagner, E.K. (1999). The polysulfonated compound suramin blocks adsorption and lateral difusion of herpes simplex virus type-1 in vero cells. *Virology*, 258(1):141-151. https://doi.org/10.1006/viro.1999.9723
5. Akhtar, J., & Shukla, D. (2009) Viral entry mechanisms: cellular and viral mediators of herpes simplex virus entry. *The FEBS Journal*, 276(24):7228-7236. https://doi.org/10.1111/j.1742-4658.2009.07402.x
6. Amorini, A. M., Giorlandino, C., Longo, S., D'Urso, S., Mesoraca, A., Santoro, M. L., … Tavazzi B (2012). Metabolic profile of amniotic fluid as a biochemical tool to screen for inborn errors of metabolism and fetal anomalies. *Molecular Cell & Biochemistry*, 359(1-2), 205–216. https://doi.org/10.1007/s11010-011-1015-y
7. Amorini, A.M., Lazzarino, G., Di Pietro, V., Signoretti, S., Lazzarino, G., Belli, A., Tavazzi B. (2017). Severity of experimental traumatic brain injury modulates changes in concentrations of cerebral free amino acids. *Journal of Cellular and Molecular Medicine*, 21(3):530-542. https://doi.org/10.1111/jcmm.12998
8. Aplin, A.E., Gibb, G.M., Jacobsen, J.S., Gallo, J.M., Anderton, B.H. (1996). In vitro phosphorylation of the cytoplasmic domain of the amyloid precursor protein by glycogen synthase kinase-3beta. *Journal of Neurochemistry*, 67(2):699-707. https://doi.org/10.1046/j.1471-4159.1996.67020699.x

9. Araque, A., Parpura, V., Sanzgiri, R.P., Haydon, P.G. (1998). Glutamate-dependent astrocyte modulation of synaptic transmission between cultured hippocampal neurons. *European Journal of Neuroscience*, 10(6):2129-2142. https://doi.org/10.1046/j.1460-9568.1998.00221.x
10. Araque, A., Carmignoto, G., Haydon, P.G., Oliet, S.H.R., Robitaille, R., Volterra, A. (2014). Gliotransmitters Travel in Time and Space. *Neuron*, 81(4): 728-739. https://doi.org/10.1016/j.neuron.2014.02.007
11. Athmanathan, S., Vydehi, B.V., Sundaram, C., Vemuganti, G.K., Murthy, J.M. (2001). Neuronal apoptosis in herpes simplex virus - 1 encephalitis (HSE). *Indian Journal of Medical Microbi*ology, 19(3):127-131.
12. Bazargani, N., & Attwell D. (2016). Astrocyte calcium signaling: the third wave. (2016). *Nature Neuroscience*, 19(2):182-189. https://doi.org/10.1038/nn.4201
13. Bender, C., Frik, J., Gòmez R.M. (2012). Role of astrocytes in viral infections. In *Astrocytes*. New York, NY: Nova Science Publisher
14. Burnstock, G. (2007). Physiology and pathophysiology of purinergic neurotransmission. *Physiology Review,* 87(2), 659–797. https://doi.org/10.1152/physrev.00043.2006
15. Casrouge, A., Zhang, S.Y., Eidenschenk, C., Jouanguy, E., Puel, A., Yang, K., … Casanova J.L. (2006). Herpes simplex virus encephalitis in human UNC-93B deficiency. *Science*, 314(5797):308-312. https://doi.org/ 10.1126/science.1128346
16. Cheshenko, N., Del Rosario, B., Woda, C., Marcellino, D., Satlin, L.M., Herold, B.C. (2003). Herpes simplex virus triggers activation of calcium-signaling pathways. *The Journal of Cell Biology*, 163(2):283-293. https://doi.org/10.1083/jcb.200301084
17. Cheshenko, N., Trepanier, J.B., Stefanidou, M., Buckley, N., Gonzalez, P., Jacobs W., Herold, B.C. (2013). HSV activates Akt to trigger calcium release and promote viral entry: novel candidate target for treatment and suppression. *The FASEB Journal*. 27(7):2584-2599. https://doi.org/10.1096/fj.12-220285

18. Cheshenko, N., Pierce, C., Herold, B.C. (2018) Herpes simplex viruses activate phospholipid scramblase to redistribute phosphatidylserines and Akt to the outer leaflet of the plasma membrane and promote viral entry. *PLoS Pathogens*. 14(1):e1006766. https://doi.org/10.1371/journal.ppat.1006766

19. Colombres, M., Henríquez, J.P., Reig, G.F., Scheu, J., Calderón, R., Alvarez, A, … Inestrosa, N.C. (2008). Heparin activates Wnt signaling for neuronal morphogenesis. Journal of Cellular Physiology, 216(3):805-815. https://doi.org/10.1002/jcp.21465

20. Cotrina, M.L., Lin, J.H., Lopez-Garcia J.C., Naus, C.C., Nedergaard, M. (2000). ATP-mediated glia signaling. *The Journal of Neuroscience*, 20(8): 2835-2844. https://doi.org/10.1523/JNEUROSCI.20-08-02835.2000

21. Clarke, D.D. (1991). Fluoroacetate and fluorocitrate: mechanism of action. *Neurochemical Research*, 16(9):1055-1058. https://doi.org/10.1007/BF00965850

22. De Chiara, G., Marcocci, M.E., Civitelli, L., Argnani, R., Piacentini, R., Ripoli, C., … Palamara, A.T. (2010). APP processing induced by herpes simplex virus type 1 (HSV-1) yields several APP fragments in human and rat neuronal cells. *PLoS One*, 5(11):e13989. https://doi.org/10.1371/journal.pone.0013989

23. De Chiara, G., Marcocci, M.E., Sgarbanti, R., Civitelli, L., Ripoli, C., Piacentini, R., … Palamara, A.T. (2012). Infectious agents and neurodegeneration. *Molecular Neurobiology*, 46(3):614-38. https://doi.org/10.1007/s12035-012-8320-7

24. De Chiara, G., Racaniello, M., Mollinari, C., Marcocci, M. E., Aversa, G., Cardinale, A., … Merlo, D. (2016). Herpes Simplex Virus-Type1 (HSV-1) Impairs DNA Repair in Cortical Neurons. *Frontiers in aging neuroscience*, 8, 242. https://doi.org/10.3389/fnagi.2016.00242

25. De Chiara, G., Piacentini, R., Fabiani, M., Mastrodonato, A., Marcocci, M.E., Limongi, D., … Palamara, A.T. (2019). Recurrent Herpes Simplex Virus-1 infection induces hallmarks of neurodegeneration and cognitive deficits in mice. *Plos Pathogens*, 15(3):e1007617. https://doi.org/10.1371/journal.ppat.1007617

26. Fields, R.D., & Burnstock, G. (2006). Purinergic signalling in neuron-glia interactions. *Nature Reviews Neuroscience*,7(6):423-436. https://doi.org/10.1038/nrn1928

27. Fumagalli, M., Brambilla, R., D'Ambrosi, N., Volonté, C., Matteoli, M, … Abbracchio, M.P. (2003). Nucleotide-mediated calcium signaling in rat cortical astrocytes: Role of P2X and P2Y receptors. *Glia*, 43(3):218-03. doi: 10.1002/glia.10248.

28. Gordon, G.R.J., Baimoukhametova, D.V., Hewitt, S.A., Rajapaksha, W.R., Fisher,T.E., Bains, J.S. (2005). Norepinephrine triggers release of glial ATP to Increase postsynaptic efficacy. *Nature Neuroscience*, 8(8): 1078-1086. https://doi.org/10.1038/nn1498

29. Goto, T., Iwai, H., Kuramoto, E., Yamanaka, A. (2017). Neuropeptides and ATP signaling in the trigeminal ganglion. *Japanese Dental Science Review*, 53(4):117-124. doi: https://doi.org/10.1016/j.jdsr.2017.01.003

30. Guendel, I., Iordanskiy, S., Van Duyne, R., Kehn-Hall, K., Saifuddin, M., Das, R, … Kashanchi, F. (2014). Novel neuroprotective GSK-3β inhibitor restricts Tat-mediated HIV-1 replication. *Journal of Virology*, 88(2):1189-1208. https://doi.org/10.1128/JVI.01940-13

31. Gulisano, W., Melone, M., Ripoli, C., Tropea, M.R., Li Puma, D.D., Giunta, S., … Puzzo, D. 2019). Neuromodulatory Action of Picomolar Extracellular Aβ42 Oligomers on Presynaptic and Postsynaptic Mechanisms Underlying Synaptic Function and Memory. *Journal of Neuroscience*, 39(30):5986-6000. https://doi.org/10.1523/JNEUROSCI.0163-19.2019

32. Halassa, M.M., & Haydon, P.G. (2010). Integrated brain circuits: astrocytic networks modulate neuronal activity and behavior. *Annual Review of Physiology*, 72: 335-355. https://doi.org/10.1146/annurev-physiol-021909-135843

33. Jourdain, P., Bergersen, L.H., Bhaukaurally, K., Bezzi, P., Santello, M., Domercq, M, … Volterra, A. (2007). Glutamate exocytosis from astrocytes controls synaptic strength. *Nature Neuroscience*, 10(3):331-339. https://doi.org/10.1038/nn1849

34. Juaristi, I., Llorente-Folch, I., Satrústegui, J., Del Arco, A. (2019). Extracellular ATP and glutamate drive pyruvate production and energy demand to regulate mitochondrial respiration in astrocytes.

Glia, 67(4):759-774. doi: 10.1002/glia.23574.

35. Kang, Y., Yuan, R., Zhao, X., Xiang, B., Gao, S., Gao, P., … Rent, T. (2017). Transient activation of the PI3K/Akt pathway promotes Newcastle disease virus replication and enhances anti-apoptotic signaling responses. *Oncotarget*, 8(14):23551-23563. https://doi.org/10.18632/oncotarget.15796
36. Kehn-Hall, K., Narayanan, A., Lundberg, L., Sampey, G., Pinkham, C., Guendel, I., … Kashanchi, F. (2012). Modulation of GSK-3β activity in Venezuelan equine encephalitis virus infection. *PLoS One*, 7(4):e34761. https://doi.org/10.1371/journal.pone.0034761
37. Killington, R.A., Powell, K.L. (1991). Growth, assay and purification of Herpes viruses. In: Mahy BWJ, editor. Virology: a Practical Approach: Oxford: IRL Press. 207-236
38. Kong, N., Wu, Y., Meng, Q., Wang, Z., Zuo, Y., Pan, X., … Tong, G. (2016). Suppression of Virulent Porcine Epidemic Diarrhea Virus Proliferation by the PI3K/Akt/GSK-3α/β Pathway. *PLoS One*, 11(8):e0161508. https://doi.org/10.1371/journal.pone.0161508
39. Lafaille, F.G., Pessach, I.M., Zhang, S.Y., Ciancanelli, M.J., Herman, M., Abhyankar, A., … Notarangelo, L.D. (2012). Impaired intrinsic immunity to HSV-1 in human iPSC-derived TLR3-deficient CNS cells. *Nature*, 491(7426):769-773. https://doi.org/10.1038/nature11583
40. Lathe, R., Haas, J.G. (2017). Distribution of cellular HSV-1 receptor expression in human brain. *Journal of Neurovirology*. 23(3):376-384. https://doi.org/10.1007/s13365-016-0504-x
41. Leone, L., Colussi, C., Gironi, K., Longo, V., Fusco, S., Li Puma, D.D., … Grassi C. (2019). Altered Nup153 Expression Impairs the Function of Cultured Hippocampal Neural Stem Cells Isolated from a Mouse Model of Alzheimer's Disease. *Molecular Neurobiology*, 56(8):5934-5949. https://doi.org/10.1007/s12035-018-1466-1
42. Li Puma, D.D., Piacentini, R., Leone, L., Gironi, K., Marcocci, M.E., De Chiara G., … Grassi C. (2019). Herpes Simplex Virus Type-1 Infection Impairs Adult Hippocampal Neurogenesis via Amyloid-β Protein Accumulation. *Stem Cells*, 37(11):1467-1480. https://doi.org/10.1002/stem.3072

43. Okubo, Y., Kanemaru, K., Suzuki, J., Kobayashi, K., Hirose, K., & Iino, M. (2019). Inositol 1,4,5-trisphosphate receptor type 2-independent Ca^{2+} release from the endoplasmic reticulum in astrocytes. *Glia*, 67(1), 113–124. https://doi.org/10.1002/glia.23531

44. Pacheco, P.A., Faria, R.X., Ferreira, L.G., Paixão, I.C. (2014). Putative roles of purinergic signaling in human immunodeficiency virus-1 infection. *Biology Direct*, 9:21. https://doi.org/10.1186/1745-6150-9-21

45. Panella, S., Marcocci, M.E., Celestino, I., Valente, S., Zwergel, C., Li Puma, D.D., … Palamara, A.T. (2016). MC1568 inhibits HDAC6/8 activity and influenza A virus replication in lung epithelial cells: role of Hsp90 acetylation. *Future Medicinal Chemistry*, 8(17):2017-2031. https://doi.org/10.4155/fmc-2016-0073

46. Phatnani, H., & Maniatis, T. (2015). Astrocytes in neurodegenerative disease. *Cold Spring Harbor Perspectives in Biology*, 15; 7(6): a020628. https://doi,org/10.1101/cshperspect.a020628

47. Piacentini, R., Gangitano, C., Ceccariglia, S., Del Fà, A., Azzena, G.B., Michetti, F., Grassi, C. (2008). Dysregulation of intracellular calcium homeostasis is responsible for neuronal death in an experimental model of selective hippocampal degeneration induced by trimethyltin. *Journal of Neurochemistry*, 105(6):2109-2121. https://doi.org/10.1111/j.1471-4159.2008.05297.x

48. Piacentini, R., Civitelli, L., Ripoli, C., Marcocci, M.E., De Chiara, G., Garaci, E., … Grassi, C. (2011). HSV-1 promotes Ca^{2+} -mediated APP phosphorylation and Aβ accumulation in rat cortical neurons. *Neurobiology of Aging*, 32(12):2323.e13-26. https://doi.org/10.1016/j.neurobiolaging.2010.06.009

49. Piacentini, R., De Chiara, G., Li Puma, D.D., Ripoli, C., Marcocci, M.E., Garaci, E., … Grassi, C. (2014). HSV-1 and Alzheimer's disease: more than a hypothesis. *Frontiers in Pharmacology*, 5:97. https://doi.org/10.3389/fphar.2014.00097

50. Piacentini, R., Li Puma, D.D., Ripoli, C., Marcocci, M.E., De Chiara, G., Garaci, E., … Grassi, C. (2015). Herpes Simplex Virus type-1 infection induces synaptic dysfunction in cultured cortical neurons via GSK-3 activation and intraneuronal amyloid-β protein accumulation. *Scientific Reports*, 5:15444. https://doi.org/10.1038/srep15444

51. Piacentini, R., Li Puma, D.D., Mainardi, M., Lazzarino, G., Tavazzi, B., Arancio, O., … Grassi, C. (2017). Reduced gliotransmitter release from astrocytes mediates tau-induced synaptic dysfunction in cultured hippocampal neurons. *Glia*, 65(8):1302-1316. https://doi.org/10.1002/glia.23163
52. Perea, G., Navarrete, M., Araque, A. (2009). Tripartite synapse: astrocytes process and control synaptic information. *Trends in Neurosciences*, 32(8):421-431. https://doi.org/10.1016/j.tins.2009.05.001
53. Perea, G., & Araque, A. (2010). GLIA modulates synaptic transmission. *Brain Research Reviews*, 63(1-2):93-102. https://doi.org/10.1016/j.brainresrev.2009.10.005
54. Pierrot, N., Santos, S.F., Feyt, C., Morel, M., Brion, J.P., Octave, J.N. (2006). Calcium-mediated transient phosphorylation of tau and amyloid precursor protein followed by intraneuronal amyloid-beta accumulation. *Journal of Biological Chemistry*, 281(52):39907-39914. https://doi.org/10.1074/jbc.M606015200
55. Qie, L., Marcellino, D., Herold, B.C. (1999). Herpes simplex virus entry is associated with tyrosine phosphorylation of cellular proteins. *Virology*, 256(2):220-227. https://doi.org/10.1006/viro.1999.9673
56. Randall, R.E., & Dinwoodie, N. (1986). Intranuclear localization of herpes simplex virus immediate-early and delayed-early proteins: evidence that ICP 4 is associated with progeny virus DNA. *Journal of general virology*, 67 (Pt 10):2163-77. https://doi.org/10.1099/0022-1317-67-10-2163
57. Sarhan, M.A., Abdel-Hakeem, M.S., Mason, A.L., Tyrrell, D.L., Houghton, M. (2017). Glycogen synthase kinase 3β inhibitors prevent hepatitis C virus release/assembly through perturbation of lipid metabolism. *Scientific Reports*, 7(1):2495. https://doi.org/10.1038/s41598-017-02648-6
58. Séror, C., Melki, M.T., Subra, F., Raza, S.Q., Bras, M., Saïdi, H., … Perfettini JL. (2011). Extracellular ATP acts on P2Y2 purinergic receptors to facilitate HIV-1 infection. *Journal of Experimental Medicine*, 208(9):1823-1834. https://doi.org/10.1084/jem.20101805

59. Sherwood, M.W., Arizono, M., Hisatsune, C., Bannai, H., Ebisui, E., Sherwood, J.L., … Mikoshiba K. (2017). Astrocytic IP3 Rs: Contribution to Ca^{2+} signalling and hippocampal LTP. *Glia*. 65(3):502-513. doi: 10.1002/glia.23107.

60. Shukla, D., & Spear, P.G. (2001). Herpesviruses and heparan sulfate: an intimate relationship in aid of viral entry. *Journal of Clinical Investigation*, 108(4):503-510. https://doi.org/10.1172/JCI13799

61. Sofroniew, M.V. (2009). Molecular dissection of reactive astrogliosis and glial scar formation. *Trends in Neurosciences*, 32(12):638-647. https://doi.org/10.1016/j.tins.2009.08.002

62. Swartz, T.H., Dubyak, G.R., Chen, B.K. (2015). Purinergic Receptors: Key Mediators of HIV-1 Infection and Inflammation. *Frontiers in Immunology*, 6:585. https://doi.org/10.3389/fimmu.2015.00585

63. Tavazzi, B., Lazzarino, G., Leone, P., Amorini, A. M., Bellia, F., Janson, C. G., … Giardina, B. (2005). Simultaneous high-performance liquid chromatographic separation of purines, pyrimidines, N-acetylated amino acids, and dicarboxylic acids for the chemical diagnosis of inborn errors of metabolism. *Clinical Biochemistry*, 38(11), 997-1008. https://doi.org/10.1016/j.clinbiochem.2005.08.002

64. Taylor, A., Harker, J.A., Chanthong, K., Stevenson, P.G., Zuniga, E.I., Rudd, C.E. (2016). Glycogen Synthase Kinase 3 Inactivation Drives T-bet-Mediated Downregulation of Co-receptor PD-1 to Enhance CD8(+) Cytolytic T Cell Responses. *Immunity*, 44(2):274-86. https://doi.org/10.1016/j.immuni.2016.01.018

65. Tiwari, V., Tarbutton, M.S., Shukla, D. (2015). Diversity of heparan sulfate and HSV entry: basic understanding and treatment strategies. *Molecules*, 20(2):2707-2727 https://doi.org/10.3390/molecules20022707

66. Tovar-Y-Romo, L.B., Kolson, D.L., Bandaru, V.V., Drewes, J.L., Graham, D.R., Haughey, N.J. (2013). Adenosine triphosphate released from HIV-infected macrophages regulates glutamatergic tone and dendritic spine density on neurons. *Journal of Neuroimmune Pharmacology*, 8(4):998-1009. https://doi.org/10.1007/s11481-013-9471-7

67. Trybala, E., Liljeqvist, J.A., Svennerholm, B., Bergström, T. (2000). Herpes simplex virus types 1 and 2 differ in their interaction with heparan sulfate. *Journal of Virology*, 74(19):9106-9114. https://doi.org/10.1128/jvi.74.19.9106-9114.2000

68. Vahlne, A., Nyström, B., Sandberg, M., Hamberger, A., Lycke, E. (1978). Attachment of herpes simplex virus to neurons and glial cells. *Journal of General Virology*, 40(2):359-371 https://doi.org/10.1099/0022-1317-40-2-359

69. Vahlne, A., Svennerholm, B., Sandberg, M., Hamberger, A., Lycke, E. (1980). Differences in attachment between herpes simplex type 1 and type 2 viruses to neurons and glial cells. *Infection and Immunity*, 28(3):675-680

70. Vastag, L., Koyuncu, E., Grady, S.L., Shenk, T.E., Rabinowitz, J.D. (2011). Divergent effects of human cytomegalovirus and herpes simplex virus-1 on cellular metabolism. *Plos Pathogens*, 7(7):e1002124. https://doi.org/10.1371/journal.ppat.1002124

71. Verkhratsky, A. (2019). Astroglial Calcium Signaling in Aging and Alzheimer's Disease. *Cold Spring Harbor Perspectives in Biology*, 11(7), pii: a035188. https://doi.org/10.1101/cshperspect.a035188

72. Voloboueva, L.A., Suh, S.W., Swanson, R.A., Giffard, R.G. (2007). Inhibition of mitochondrial function in astrocytes: implications for neuroprotection. *Journal of Neurochemistry*, 102(4):1383-1394. https://doi.org/10.1111/j.1471-4159.2007.04634.x

73. Volterra, A., & Meldolesi, J. (2005). Astrocytes, from brain glue to communication elements: the revolution continues. *Nature Reviews Neuroscience*, 6(8),626-640. https://doi.org/10.1038/nrn1722

74. Volterra, A., Liaudet, N., Savtchouk, I. (2014). Astrocyte Ca^{2+} signalling: an unexpected complexity. *Nature Reviews Neuroscience*, 15(5):327-335. https://doi.org/10.1038/nrn3725

75. Von Kügelgen I, & Hoffmann, K. (2016). Pharmacology and structure of P2Y receptors. *Neuropharmacology*, 104:50-61. https://doi.org/10.1016/j.neuropharm.2015.10.030

76. Wang, Z., Haydon P.G., Yeung, E.S. (2000). Direct observation of calcium-independent intercellular ATP signaling in astrocytes. *Analytic Chemistry*, 72(9): 2001-2007

https://doi.org/10.1021/ac9912146

77. Warwick, R.A., & Hanani, M. (2016). Involvement of aberrant calcium signalling in herpetic neuralgia. *Experimental Neurology*, 277:10-18. https://doi.org/10.1016/j.expneurol.2015.12.002
78. Wilkinson, R., Leaver, C., Simmons, A., Pereira, R.A. (1999). Restricted replication of herpes simplex virus in satellite glial cell cultures clonally derived from adult mice. *Journal of NeuroVirology*, 5(4):384-391. https://doi.org/10.3109/13550289909029479
79. Wu, C.H., Yeh, S.H., Tsay, Y.G., Shieh, Y.H., Kao, C.L., Chen, Y.S., … Chen, P.J. (2009). Glycogen synthase kinase-3 regulates the phosphorylation of severe acute respiratory syndrome coronavirus nucleocapsid protein and viral replication. *Journal of Biological Chemistry*, 284(8):5229-5239. https://doi.org/10.1074/jbc.M805747200
80. Zerboni, L., Che, X., Reichelt, M., Qiao, Y., Gu, H., Arvin, A. (2013). Herpes simplex virus 1 tropism for human sensory ganglion neurons in the severe combined immunodeficiency mouse model of neuropathogenesis. *Journal of Virology*, 87(5):2791-2802. https://doi.org/10.1128/JVI.01375-12. 26
81. Zonta, M., & Carmignoto, G. (2002). Calcium oscillations encoding neuron-to-astrocyte communication. Journal of Physiology Paris, 96(3-4):193-198. https://doi.org/10.1016/S0928-4257(02)00006-2
82. Zorec, R., Parpura, V., Verkhratsky, A. (2017). Astroglial Vesicular Trafficking in Neurodegenerative Diseases. *Neurochemical Research*, 42(3):905-917. https://doi.org/10.1007/s11064-016-2055-1

Figure Legends

Figure 1. Neurons in the proximity of HSV-1-infected astrocytes are more susceptible to be infected by HSV-1. (a-c) Representative examples of co-cultures of mouse cortical neurons and astrocytes infected with HSV-1. Infected neurons (MAP2 positive, green) and astrocytes (MAP2 negative) were recognized by their immunoreactivity for the anti-HSV-1 antibody (red). Viewfinder allowed us to evaluate the distance of neurons from the nearest infected astrocyte. **(d)** Plot showing the percentage of infected (HSV-1-positive) and uninfected (HSV-1-negative) neurons as a function of the distance from the nearest infected astrocyte. **(e)** Bar graph showing the mean distance of HSV-1-positive and HSV-1-negative neurons from the nearest infected astrocytes. ***p<0.001.

Figure 2. FC treatment reduces the HSV-1 infection in co-cultures of neurons and astrocytes. (a) Western blot analysis carried out on lysates of co-cultures of neurons and astrocytes challenged with vehicle (lane on the left) or HSV-1 (middle lane), or treated with the astrocyte metabolism inhibitor FC (200 µM; lane on the right) 30 min before and during all the time of virus adsorption (1-hour lasting). Experiments were performed 24 h p.i.. Lysates were probed with an antibody recognizing various viral proteins (anti HSV-1). Tubulin or GAPDH were used as loading control. Red arrowhead likely corresponds to viral glycoproteins gC and gB and/or some ICPs (e.g. ICP8). **(b)** Densitometric analysis of Western blot experiment carried out in (a). **(c)** Bar graph showing mean viral titre in the supernatants of infected co-cultures of neurons and astrocytes treated or not with FC, and evaluated 24 h p.i.; *n*=18 independent experiments for HSV-1 and *n*=7 for HSV-1 with FC. **p≤0.005 *vs*. FC-untreated HSV-1. **(d)** Mean time course of intracellular Ca^{2+} signals triggered by HSV-1 (5 MOI) exposure in neurons in co-cultures treated (with; *n*=50) or not (w/o; *n*=88) with 200 µM FC. **(e)** Bar graph showing the mean peak amplitude of intracellular Ca^{2+} transients induced by extracellular application of 50 mM KCl in the same neurons in co-cultures as in (d). n.s. means not significant difference.

Figure 3. Astrocytes express more HSPGs for HSV-1 binding than neurons. (a, b) Representative examples of confocal images of $GFAP^+$ astrocytes (a_1) and $MAP2^+$ neurons (b_1) immunostained for anti-HSPGs. DAPI was used to identify cell nuclei. **(c)** Bar graph showing the relative HSPG expression, for unit of area, of neurons and astrocytes (*n*=23 for both) in culture. Scale bar: 20 µm. *p<0.05.

Figure 4. Challenge of cultured astrocytes with HSV-1 increases intracellular Ca^{2+} transients and the release of ATP. (a) Representative example of time course of intracellular Ca^{2+} transients in cultured cortical astrocytes challenged with HSV-1 (5 MOI). Different colors refer to different astrocytes. **(b, c)** Bar graphs

showing the mean values of frequency (b) and amplitude (c) of Ca^{2+} transients before (pre) and after (post) HSV-1 application. **(d)** Bar graph summarizing the amount of some gliotransmitters released in the culture medium of astrocytes during 1-h treatment with vehicle (white bar) and HSV-1 (red bar). *p<0.05; **p<0.01; ***p<0.001.

Figure 5. Addition of ATP to the culture medium of FC-treated co-cultures of neurons and astrocytes restores the virus ability to infect neurons. (a, b) Representative examples of cortical co-cultures of neurons and FC-inhibited astrocytes that were exposed (b) or not (a) to 100 µM ATP during the adsorption period of the virus. **(c)** Bar graph showing the percentage of ICP4^{+} neurons on the total in FC-treated co-cultures 24 h p.i. in the presence or not of extracellular ATP. **(d)** Representative Western blot analysis of anti-HSV-1 performed on cell lysates in the same experimental conditions described in (a-c). Tubulin was used as loading control. **(e)** Densitometric analysis of Western blot experiments shown in (d). **(f)** Bar graph showing the viral titre evaluated 24 h p.i. in the supernatants of HSV-1-infected co-cultures of neurons and astrocytes treated with either vehicle or FC (200 µM) in the presence or not of extracellular ATP (100 µM) during the adsorption period (*n*=7 independent experiments for each experimental condition). Scale bar: 10 µm. **p≤0.005 *vs*. HSV-1; #p<0.05 and ##p<0.005 *vs*. HSV-1+ FC.

Figure 6. HSV-1 induces astrocyte-mediated, purinergic receptors-dependent activation of GSK-3. (a, b) Representative examples of GFAP-positive astrocytes (red) immunoreactive for GSK-3α/β phosphorylated at Tyr279/216 (pGSK-3; green), challenged for 10 min with vehicle (a) or HSV-1 (5 MOI, b). **(c)** Cell treatment with the P2R blocker suramin (200 µM) significantly reduced the effects of HSV-1 on pGSK-3 immunoreactivity. **(d)** Bar graph showing the mean pGSK-3 immunoreactivity in the same conditions represented in a-c (*n*=174, 176 and 158 studied cells, respectively). **(e, f)** Representative examples of MAP2-positive neurons (red) immunoreactive for pGSK-3 (green) challenged for 10 min with vehicle (e) or HSV-1 particles (5 MOI, f). **(g, h)** Cell treatment with the P2R blocker suramin (200 µM, g) or the blocker of astrocyte metabolism, fluorocitric acid (FC, h), significantly reduced the effects of HSV-1 on pGSK-3 immunoreactivity. **(i)** Bar graph showing the mean pGSK-3 immunoreactivity in the conditions represented in e-h and after cell treatment with the IP_3R blocker 2-APB (*n*=297, 448, 176, 168 and 193, respectively). **(j)** Western blot analysis of pGSK-3α/β at Y276/216 and total GSK-3β in cultured cortical HSV-1-infected cells (left lane), in the presence of either FC (middle lane), or suramin (right lane). **(k)** Densitometric analysis of GSK-3β (47 kDa) protein expression in the experimental conditions shown in j. **p<0.001 *vs*. mock-infected condition; #p<0.05 and ##p<0.001 *vs*. HSV-1-infected condition. §p<0.05 *vs*. SB216763 during adsorption period. Scale bars: 10 µm.

Figure 7. GSK-3 activation is necessary for viral infection and replication. (a-c) Representative examples of immunofluorescence experiments performed with anti-HSV-1 on co-cultures of neurons and astrocytes infected with HSV-1 alone (a), or in the presence of the GSK-3 inhibitor SB216763 applied either only during the adsorption period (b), or only during the p.i. period (c). Immunoreactivity for HSV-1 was evaluated 24h p.i.. **(d)** Bar graph showing the mean viral titre in the conditions represented in a-c. **(e)** Representative Western blot analysis carried out on lysates of co-cultures of neurons and astrocytes mock-infected (left lane) or infected with HSV-1 (5 MOI) without (middle lane) or with cell treatment with SB216763 only during the adsorption period (right lane) and evaluated 24 h p.i.. Lysates were probed with anti ICP4 antibody. Red arrowhead indicates band corresponding to ICP4. GAPDH was used as loading control. **(f)** Bar graph quantifying the mean ICP4 optical density in the conditions represented in (e). *$p<0.05$ *vs*. mock-infected condition. #$p<0.05$ *vs*. HSV-1-infected condition. §$p<0.05$ *vs*. SB216763 during adsorption period. Scale bars: 50 µm.

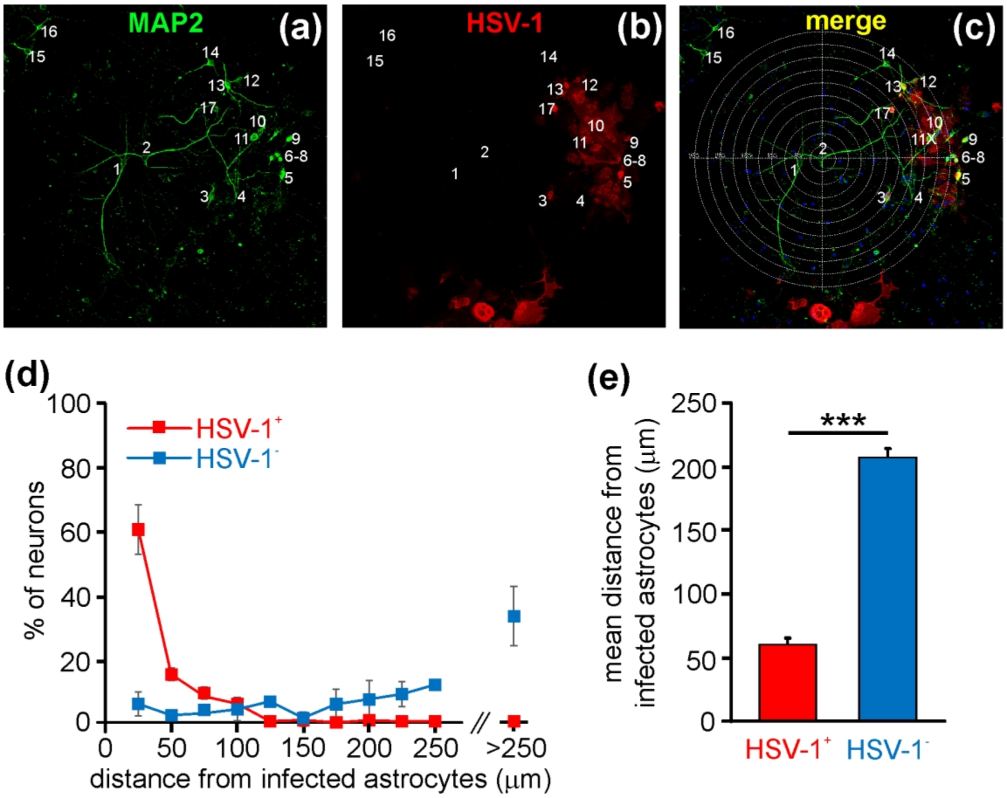

Figure 1. Neurons in the proximity of HSV-1-infected astrocytes are more susceptible to be infected by HSV-1. (a-c) Representative examples of co-cultures of mouse cortical neurons and astrocytes infected with HSV-1. Infected neurons (MAP2 positive, green) and astrocytes (MAP2 negative) were recognized by their immunoreactivity for the anti-HSV-1 antibody (red). Viewfinder allowed us to evaluate the distance of neurons from the nearest infected astrocyte. **(d)** Plot showing the percentage of infected (HSV-1-positive) and uninfected (HSV-1-negative) neurons as a function of the distance from the nearest infected astrocyte. **(e)** Bar graph showing the mean distance of HSV-1-positive and HSV-1-negative neurons from the nearest infected astrocytes. ***p<0.001.

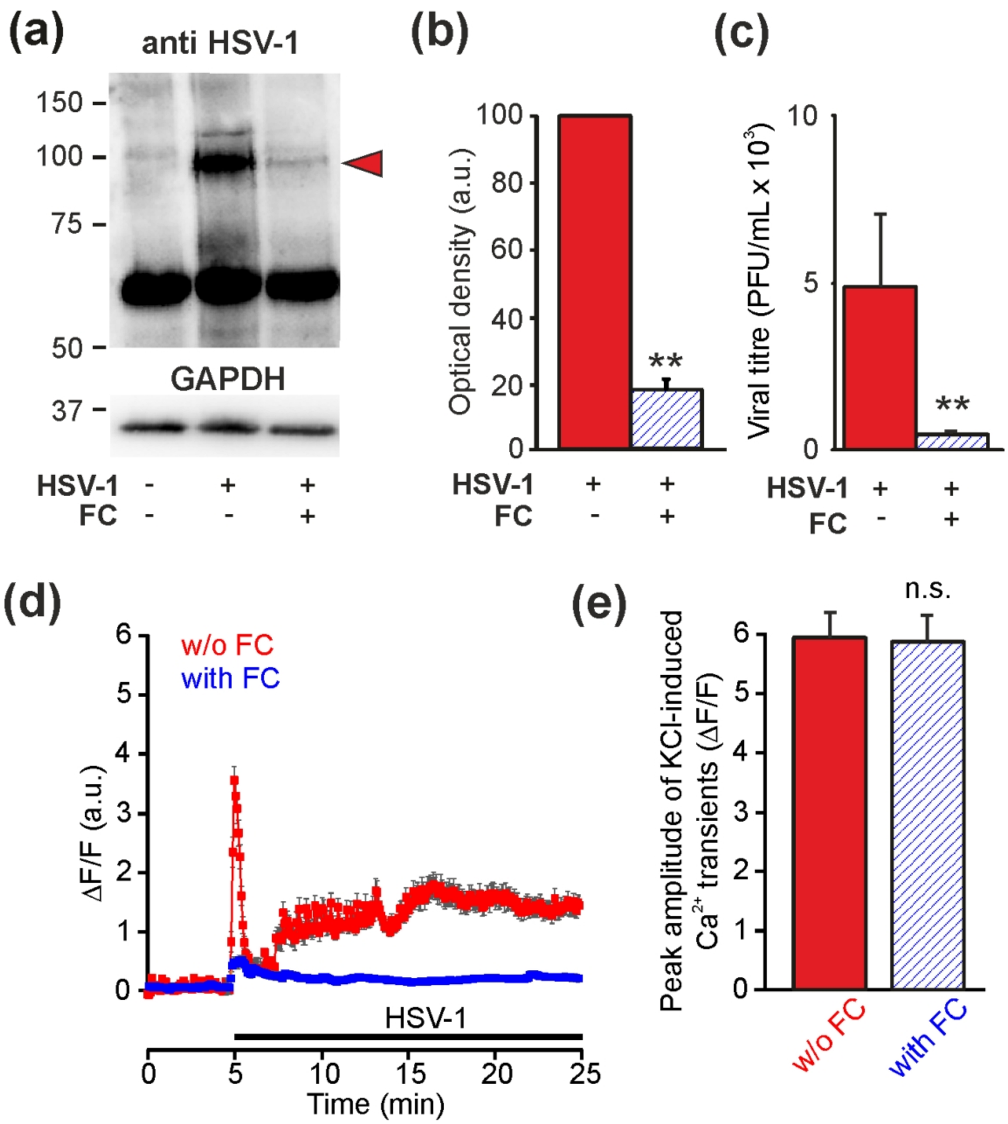

Figure 2. FC treatment reduces the HSV-1 infection in co-cultures of neurons and astrocytes. (a) Western blot analysis carried out on lysates of co-cultures of neurons and astrocytes challenged with vehicle (lane on the left) or HSV-1 (middle lane), or treated with the astrocyte metabolism inhibitor FC (200 μM; lane on the right) 30 min before and during all the time of virus adsorption (1-hour lasting). Experiments were performed 24 h p.i.. Lysates were probed with an antibody recognizing various viral proteins (anti HSV-1). Tubulin or GAPDH were used as loading control. Red arrowhead likely corresponds to viral glycoproteins gC and gB and/or some ICPs (e.g. ICP8). **(b)** Densitometric analysis of Western blot experiment carried out in (a). **(c)** Bar graph showing mean viral titre in the supernatants of infected co-cultures of neurons and astrocytes treated or not with FC, and evaluated 24 h p.i.; *n*=18 independent experiments for HSV-1 and *n*=7 for HSV-1 with FC. **$p \leq 0.005$ *vs.* FC-untreated HSV-1. **(d)** Mean time course of intracellular Ca^{2+} signals triggered by HSV-1 (5 MOI) exposure in neurons in co-cultures treated (with; *n*=50) or not (w/o; *n*=88) with 200 μM FC. **(e)** Bar graph showing the mean peak amplitude of intracellular Ca^{2+} transients induced by extracellular application of 50 mM KCl in in neurons in co-cultures as in (d). n.s. means not significant difference.

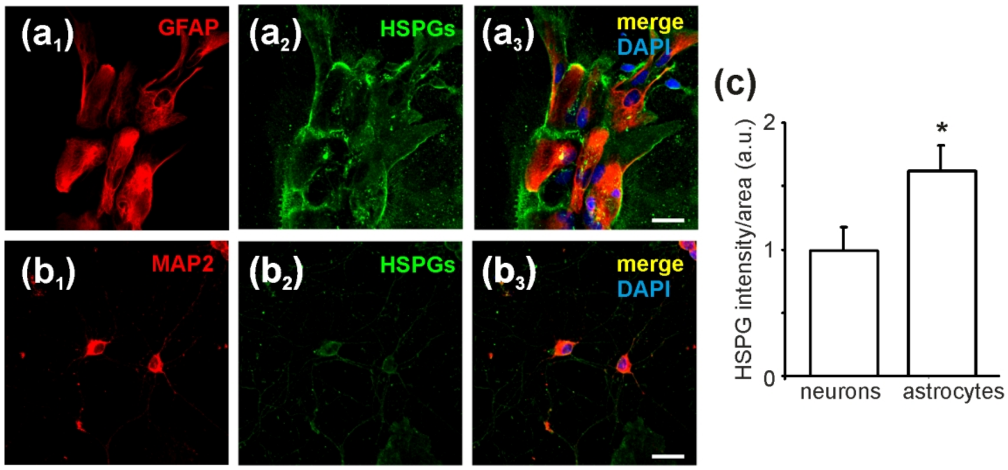

Figure 3. Astrocytes express more HSPGs for HSV-1 binding than neurons. (a, b) Representative examples of confocal images of GFAP+ astrocytes (a_1) and MAP2+ neurons (b_1) immunostained for anti-HSPGs. DAPI was used to identify cell nuclei. **(c)** Bar graph showing the relative HSPG expression, for unit of area, of neurons and astrocytes (*n*=23 for both) in culture. Scale bar: 20 μm. *p<0.05.

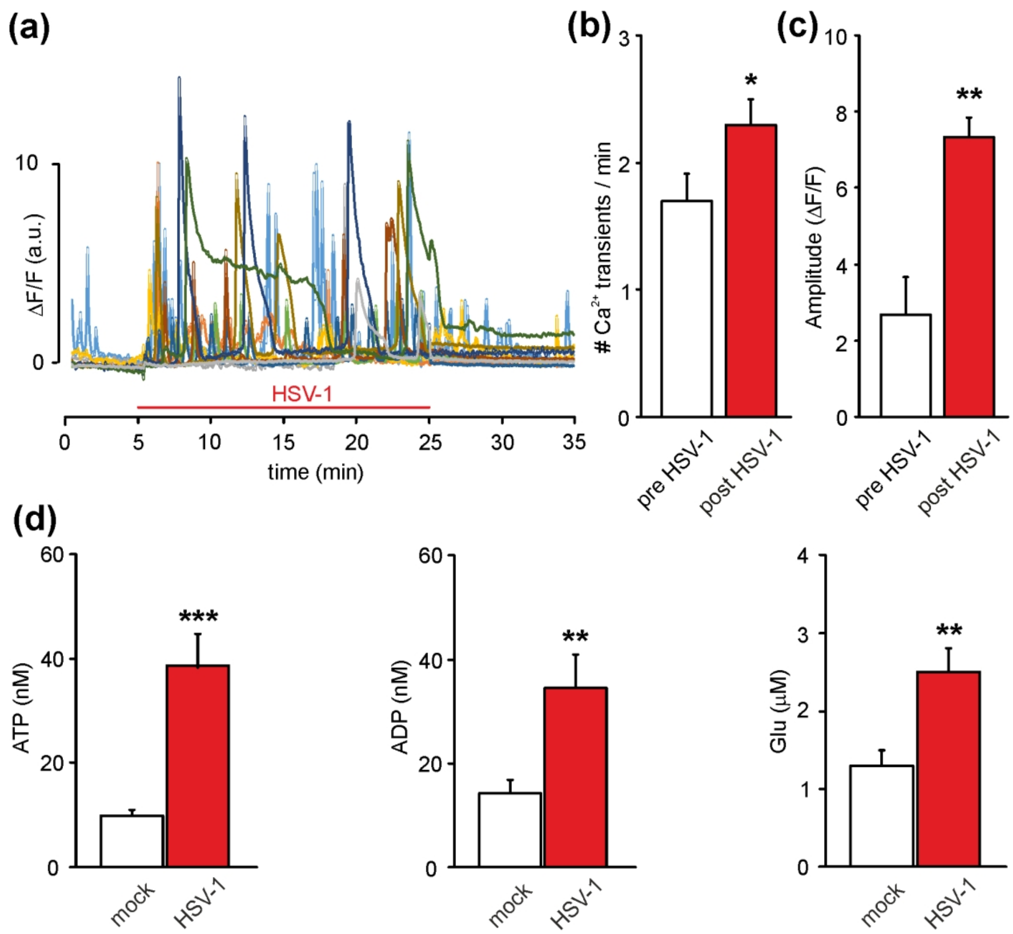

Figure 4. Challenge of cultured astrocytes with HSV-1 increases intracellular Ca^{2+} transients and the release of ATP. (a) Representative example of time course of intracellular Ca^{2+} transients in cultured cortical astrocytes challenged with HSV-1 (5 MOI). Different colors refer to different astrocytes. **(b, c)** Bar graphs showing the mean values of frequency (b) and amplitude (c) of Ca^{2+} transients before (pre) and after (post) HSV-1 application. **(d)** Bar graph summarizing the amount of some gliotransmitters released in the culture medium of astrocytes during 1-h treatment with vehicle (white bar) and HSV-1 (red bar). $^{*}p<0.05$; $^{**}p<0.01$; $^{***}p<0.001$.

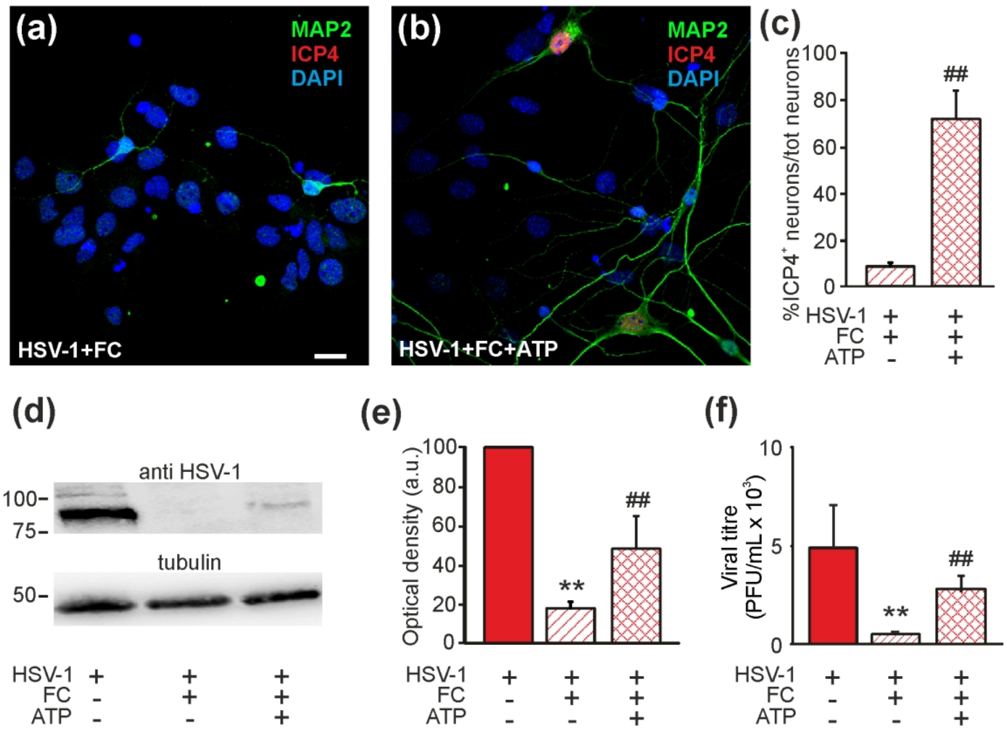

Figure 5. Addition of ATP to the culture medium of FC-treated co-cultures of neurons and astrocytes restores the virus ability to infect neurons. (a, b) Representative examples of cortical co-cultures of neurons and FC-inhibited astrocytes that were exposed (b) or not (a) to 100 μM ATP during the adsorption period of the virus. **(c)** Bar graph showing the percentage of ICP4$^+$ neurons on the total in FC-treated co-cultures 24 h p.i. in the presence or not of extracellular ATP. **(d)** Representative Western blot analysis of anti-HSV-1 performed on cell lysates in the same experimental conditions described in (a-c). Tubulin was used as loading control. **(e)** Densitometric analysis of Western blot experiments shown in (d). **(f)** Bar graph showing the viral titre evaluated 24 h p.i. in the supernatants of HSV-1-infected co-cultures of neurons and astrocytes treated with either vehicle or FC (200 μM) in the presence or not of extracellular ATP (100 μM) during the adsorption period (*n*=7 independent experiments for each experimental condition). Scale bar: 10 μm. **p≤0.005 *vs.* HSV-1; #p<0.05 and ##p<0.005 *vs.* HSV-1+ FC.

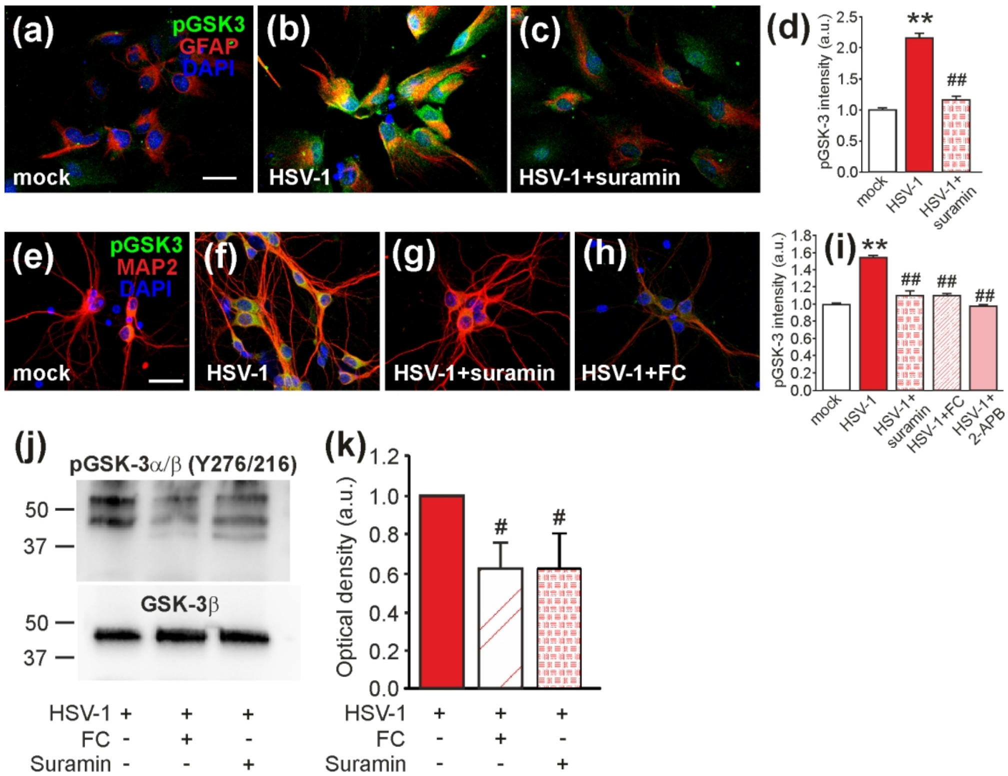

Figure 6. HSV-1 induces astrocyte-mediated, purinergic receptors-dependent activation of GSK-3. (a, b) Representative examples of GFAP-positive astrocytes (red) immunoreactive for GSK-3α/β phosphorylated at Tyr279/216 (pGSK-3; green), challenged for 10 min with vehicle (a) or HSV-1 (5 MOI, b). **(c)** Cell treatment with the P2R blocker suramin (200 μM) significantly reduced the effects of HSV-1 on pGSK-3 immunoreactivity. **(d)** Bar graph showing the mean pGSK-3 immunoreactivity in the same conditions represented in a-c (*n*=174, 176 and 158 studied cells, respectively). **(e, f)** Representative examples of MAP2-positive neurons (red) immunoreactive for pGSK-3 (green) challenged for 10 min with vehicle (e) or HSV-1 particles (5 MOI, f). **(g, h)** Cell treatment with the P2R blocker suramin (200 μM, g) or the blocker of astrocyte metabolism, fluorocitric acid (FC, h), significantly reduced the effects of HSV-1 on pGSK-3 immunoreactivity. **(i)** Bar graph showing the mean pGSK-3 immunoreactivity in the conditions represented in e-h and after cell treatment with the IP_3R blocker 2-APB (*n*=297, 448, 176, 168 and 193, respectively). **(j)** Western blot analysis of pGSK-3α/β at Y276/216 and total GSK-3β in cultured cortical HSV-1-infected cells (left lane), in the presence of either FC (middle lane), or suramin (right lane). **(k)** Densitometric analysis of GSK-3β (47 kDa) protein expression in the experimental conditions shown in j. **p<0.001 *vs.* mock-infected condition; #p<0.05 and ##p<0.001 *vs.* HSV-1-infected condition. §p<0.05 *vs.* SB216763 during adsorption period. Scale bars: 10 μm

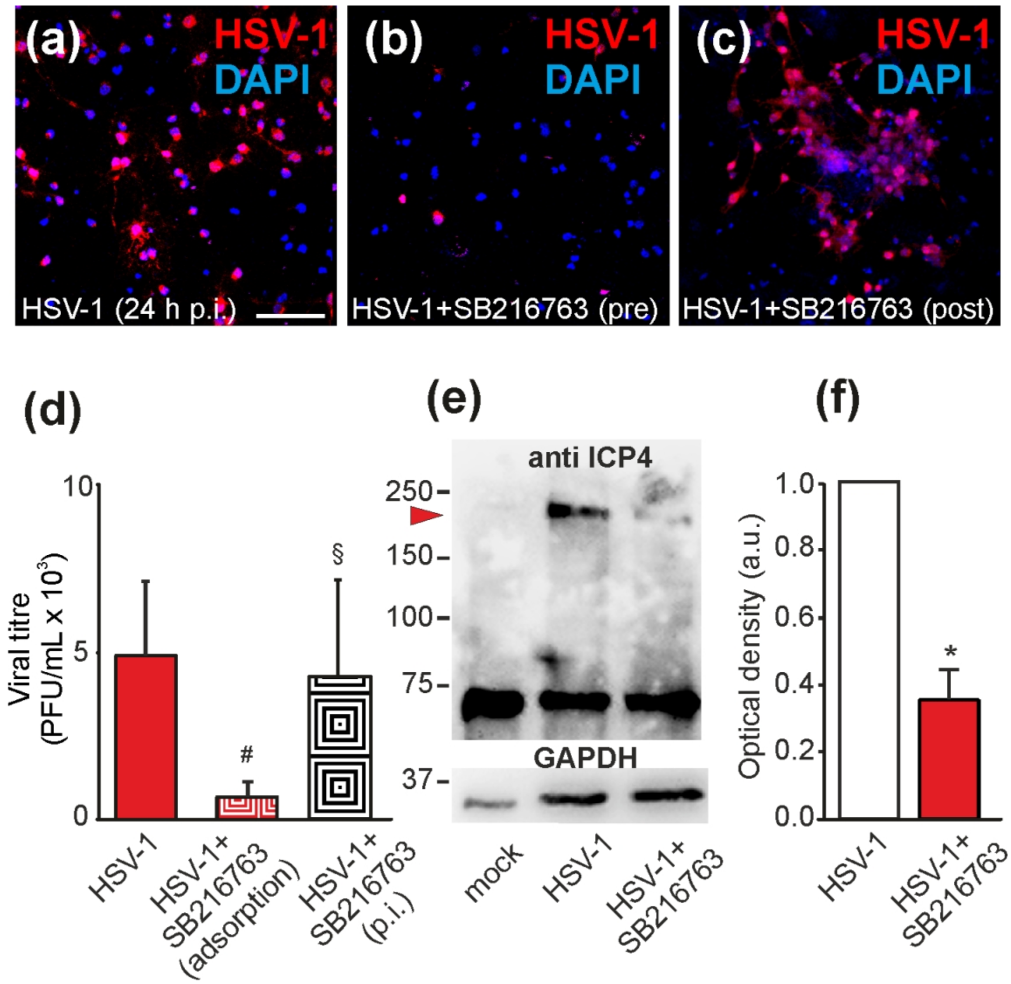

Figure 7. GSK-3 activation is necessary for viral infection and replication. (a-c) Representative examples of immunofluorescence experiments performed with anti-HSV-1 on co-cultures of neurons and astrocytes infected with HSV-1 alone (a), or in the presence of the GSK-3 inhibitor SB216763 applied either only during the adsorption period (b), or only during the p.i. period (c). Immunoreactivity for HSV-1 was evaluated 24h p.i.. **(d)** Bar graph showing the mean viral titre in the conditions represented in a-c. **(e)** Representative Western blot analysis carried out on lysates of co-cultures of neurons and astrocytes mock-infected (left lane) or infected with HSV-1 (5 MOI) without (middle lane) or with cell treatment with SB216763 only during the adsorption period (right lane) and evaluated 24 h p.i.. Lysates were probed with anti ICP4 antibody. Red arrowhead indicates band corresponding to ICP4. GAPDH was used as loading control. **(f)** Bar graph quantifying the mean ICP4 optical density in the conditions represented in (e). *p<0.05 *vs.* mock-infected condition. #p<0.05 *vs.* HSV-1-infected condition. §p<0.05 *vs.* SB216763 during adsorption period. Scale bars: 50 μm.

Supplementary Figures

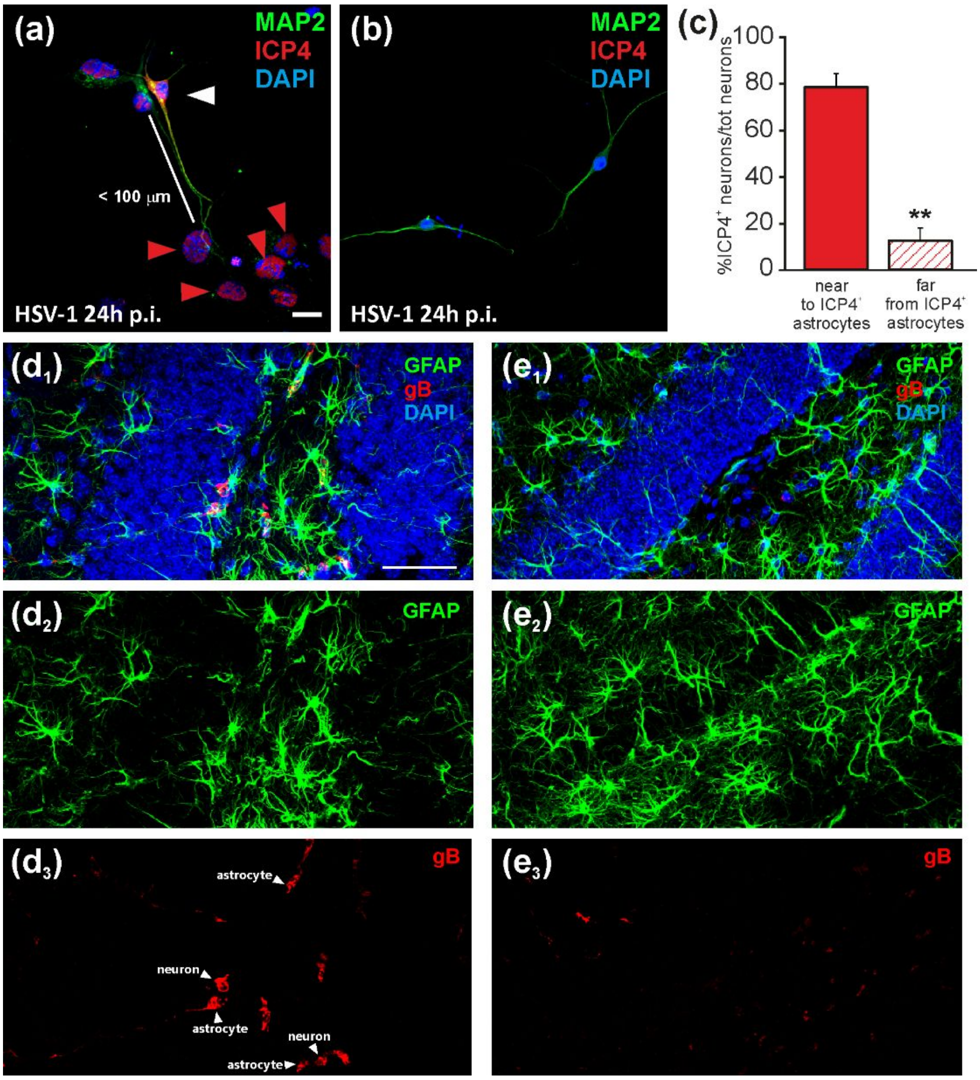

Supplementary Figure 1. Neurons in the proximity of HSV-1-infected astrocytes are more susceptible to be infected by HSV-1. (a) Representative example of cultured mouse cortical neurons (identified by MAP2 immunoreactivity and indicated with the white arrowhead) near (<100 μm) to HSV-1-infected astrocytes (MAP2-negative and ICP4-positive cells, red arrowheads). **(b)** Representative MAP2-positive neurons in the same culture as in (a) that are far (>200 μm) from infected astrocytes, i.e., neurons that are enclosed within an area lacking infected astrocytes. **(c)** Bar graph showing the percentage of ICP4-positive neurons on the total neurons that were either near to or far from infected astrocytes. **(d, e)** Representative images of coronal brain slices of hippocampal dentate gyrus from HSV-1-infected mice immunoprocessed with antibody against GFAP (in green) and gB (in red) and stained with DAPI (blue) to detect cell nuclei; d_1 and e_1 are the merged images of d_2-d_3 and e_2-e_3, respectively. Arrowheads in d_3 indicates the gB-positive granular neurons near to gB-positive astrocytes. No gB-positive neurons were found in the absence of gB-positive astrocytes (e_3). **p<0.005 *vs*. mock. Scale bars: 10 μm for panels a and b and 100 μm for panels d and e.

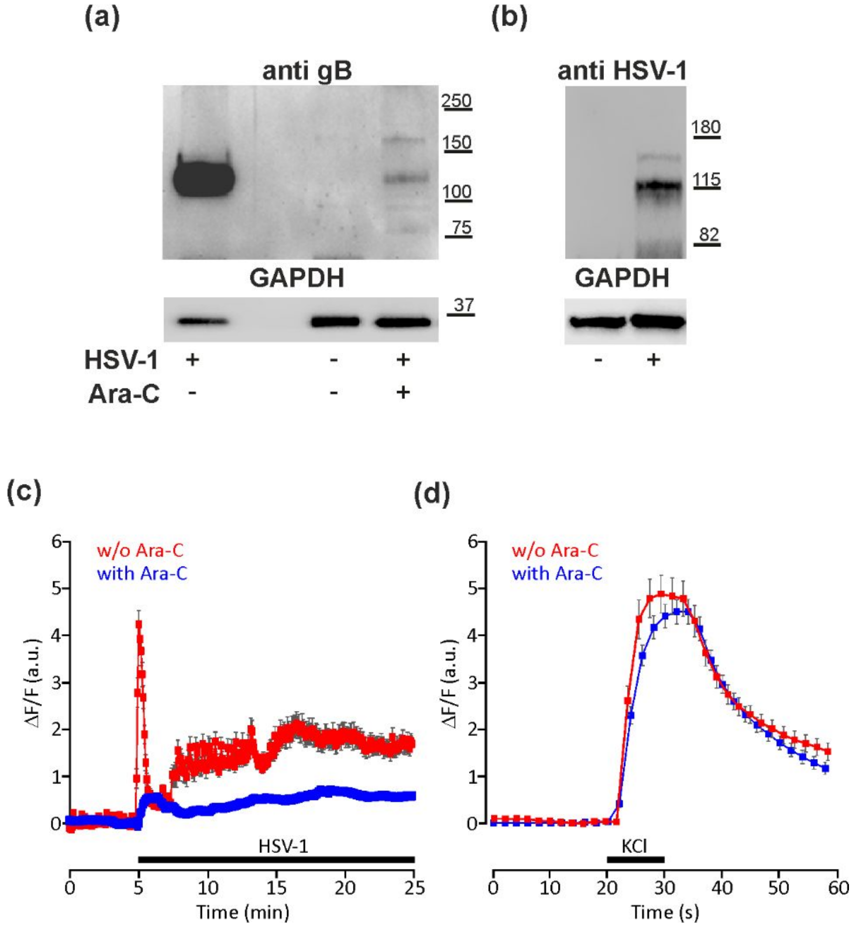

Supplementary Figure 2. Neurons grown in the absence of glial cells are less prone to be infected by HSV-1. (a) Representative Western blot (WB) analysis of anti-gB performed 24 h p.i. on lysates from mock- (middle lane) and HSV-1-infected co-culture of neurons and astrocytes treated or not (right and left lane, respectively) with 2 µM Ara-C. **(b)** Representative WB experiment of anti HSV-1 performed 24 h p.i. on primary culture of astrocytes. GAPDH was used as loading control. **(c)** Mean time course of intracellular Ca^{2+} signals triggered in neurons (recognized by their morphology) by HSV-1 exposure in co-cultures treated (with, blue line) or not (w/o, red line) Ara-C. **(d)** Time course of intracellular Ca^{2+} signals triggered by membrane depolarization obtained with extracellular application of 50 mM KCl in neurons in co-cultures treated (with, blue line; *n*=57) or not (w/o, red line; *n*=88) with 2 µM Ara-C.

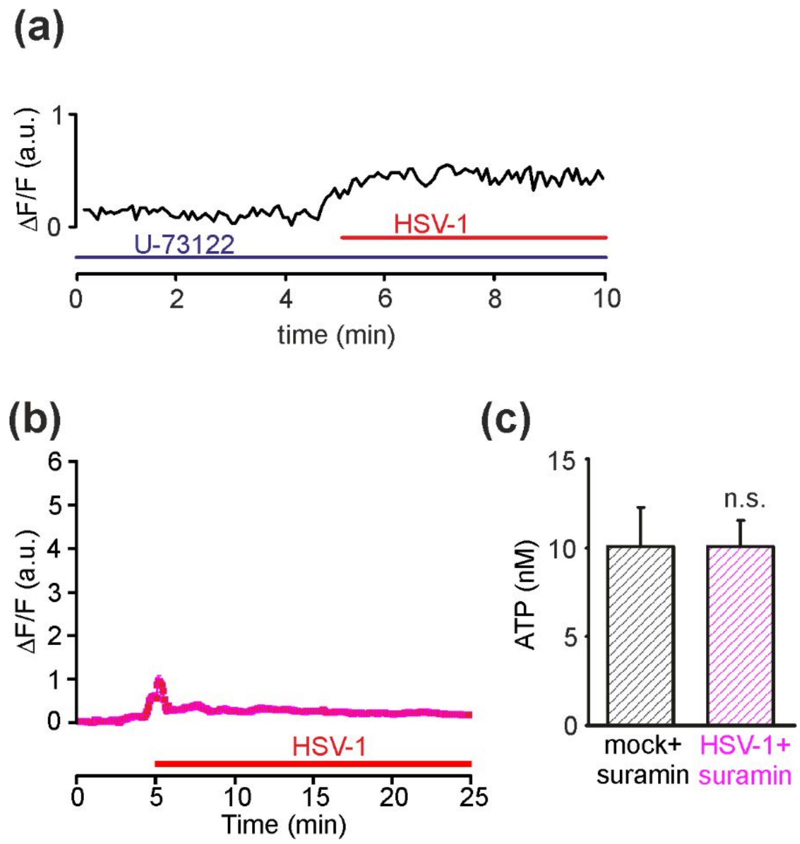

Supplementary Figure 3. Activation of P2Y receptors is involved in HSV-1-induced Ca^{2+}-dependent release of ATP. (a) Representative example of HSV-1-induced Ca^{2+} signals in cultured astrocytes treated with the PLC-inhibitor U-73122 (5 µM). **(b)** Mean time course of intracellular Ca^{2+} signals triggered in astrocytes (recognized by their morphology; *n*=37) by HSV-1 exposure in co-cultures treated with the P2R blocker suramin (200 µM). **(c)** Bar graph showing the ATP levels after treatment with 200 µM suramin in mock- and HSV-1- challenged astrocytes. n.s. means not significant difference.

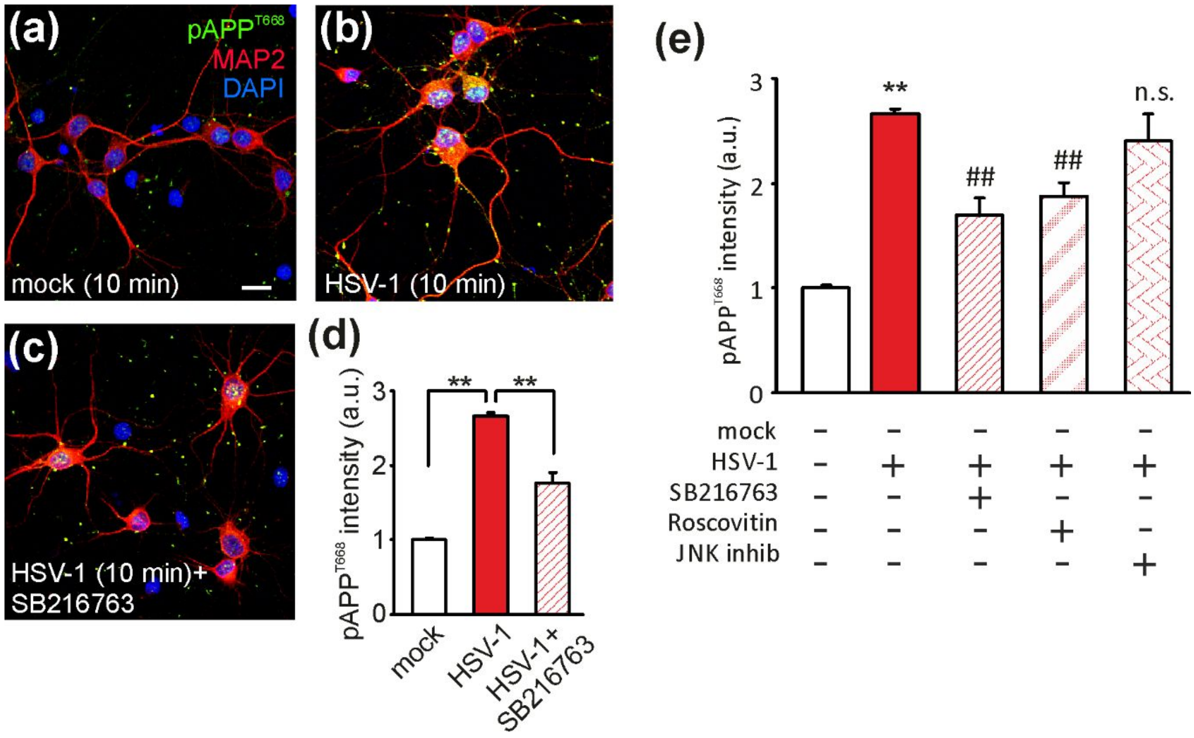

Supplementary Figure 4. HSV-1-induced APP phosphorylation at Thr668 depends on GSK-3 activation. (a, b) Representative examples of pAPP^{T668} immunoreactivity (green) in neurons challenged for 10 min with either vehicle (mock, a) or HSV-1 (5 MOI, b). **(c)** The presence of the selective GSK-3 inhibitor SB216763 (10 µM) in the culture medium significantly reduced pAPP immunoreactivity in HSV-1-challenged cells. **(d)** Bar graphs showing mean pAPP fluorescence intensity in the conditions represented in a-c. **(e)** Bar graph showing pAPP^{T668} intensity in cells treated with different kinase inhibitors. Scale bar: 10 µm. **$p<0.005$ *vs.* mock $^{\#\#}p<0.005$ *vs*. HSV-1. n.s. means not significant difference.

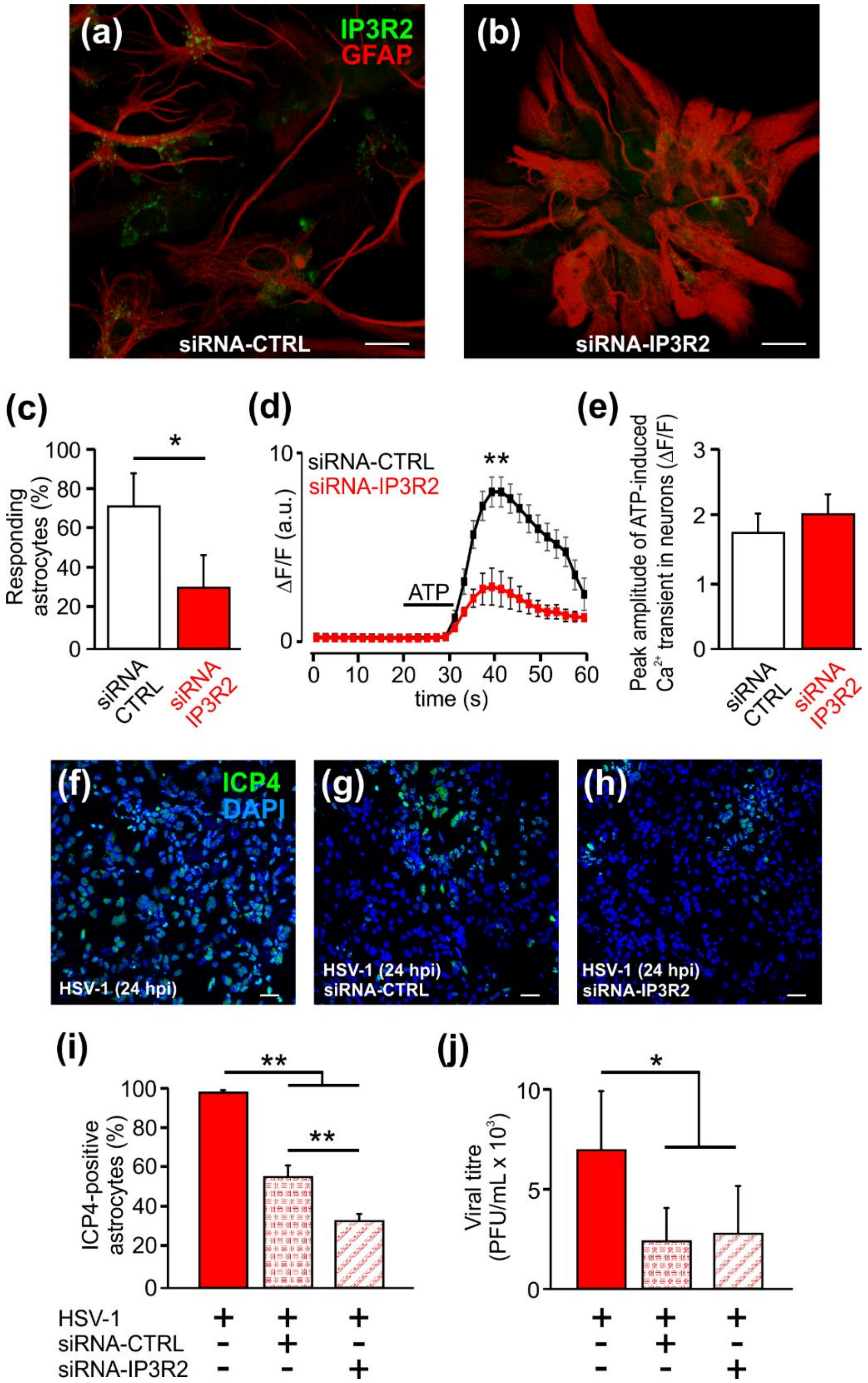

Supplementary Figure siRNA-IP3R2 interference: (a,b) Representative confocal images of IP3R2 staining in murine cultured cortical astrocytes in co-culture with neurons. The transfection efficiency was of 65.2±17.2%. Silencing reduced IP3R2 labeling in astrocytes (b) respect to vehicle alone (a). **(c-e)** Ca^{2+} imaging studies confirmed the IP3R2 silencing. In fact, the percentage of siRNA-IP3R2-transfected astrocytes responding to ATP (100 µM) stimulation applied in a solution containing 0 mM external $Ca^{2+}$was significantly reduced by 56% (c), as well as the mean amplitude of ATP-induced Ca^{2+} transients (d). In neurons, siRNA-interference had no effects (e). **(f-h)** Confocal images of HSV-1-infected cultures (24 hpi) immunoprocessed for ICP4: HSV-1 alone (f); HSV-1 in the presence of siRNA-CTRL (g); HSV-1 in the presence of siRNA-IP3R2 (h). **(i,j)** Bar graphs showing the percentage of ICP4-positive cells (h) and viral titres (i) in the conditions represented in (e-g). Scale bars: 20 µm for panels (a,b) and 50 µm for panels (f-h). * $p<0.05$; ** $p<0.001$.